DECELLULARIZATION AND CHARACTERIZATION OF LEEK: A POTENTIAL CELLULOSE-BASED BIOMATERIAL

by

Melis Toker

B.S., in Chemical Engineering, Marmara University, 2017

Submitted to the Institute of Biomedical Engineering
in partial fulfillment of the requirements
for the degree of
Master of Science
in
Biomedical Engineering

Boğaziçi University
2020

DECELLULARIZATION AND CHARACTERIZATION OF LEEK: A POTENTIAL CELLULOSE-BASED BIOMATERIAL

APPROVED BY:

Assoc. Prof. Dr. Bora Garipcan .....
(Thesis Advisor)

Assist. Prof. Dr. Duygu Ege .....

Assoc. Prof. Dr. Sedat Odabaş .....

DATE OF APPROVAL: 26 July 2019

ACKNOWLEDGMENTS

Firstly, I would like to express my utmost appreciation and sincere gratitude to my thesis advisor Assoc. Prof. Dr. Bora Garipcan for his guidance and endless support both scientifically and morally.

I thank my friend and mentor Sabra Rostami for sharing me her knowledge and experiences throughout this project. I especially thank Berkay Erenay and Burak Altun for their friendship and everything we have shared together. I also thank to Alp Özgün, Sezin Eren and all my laboratory colleagues for their support.

This project is supported by Boğaziçi University Research Fund by Grant Number No.6701.

I am grateful to my mother and my brother for believing and encouraging me to achieve what I want to do in my life.

I am deeply appreciative to Deniz Bayraktar for being always there for me with his endless love, encouragement, patience and support whenever I needed.

Finally, I dedicate this thesis to the loving memory of my father who is the reason for who I am today.

ACADEMIC ETHICS AND INTEGRITY STATEMENT

I, Melis Toker, hereby certify that I am aware of the Academic Ethics and Integrity Policy issued by the Council of Higher Education (YÖK) and I fully acknowledge all the consequences due to its violation by plagiarism or any other way.

Name :

Signature:

Date:

ABSTRACT

DECELLULARIZATION AND CHARACTERIZATION OF LEEK: A POTENTIAL CELLULOSE-BASED BIOMATERIAL

The main purpose of tissue engineering is to regenerate damaged tissues by using three-dimensional (3D) scaffolds, which mimic the *in vivo* cellular milieu. Currently scaffolds are obtained from human donors or animal products however, the need exceeds the availability. Recently, cellulose-based scaffolds, which are easily attainable biomaterials in nature, have been studied in terms of comptaibility with various mammalian cell lines. These studies have shown that plant-derived scaffolds have great potential for numerous tissue-engineering applications such as wound healing, cardiac and neural tissue engineering. In this study, leek was chosen as a model plant tissue due to its structural morphology (interconnected and elongated channel like structural morphology) as a potential 3D scaffold for tissue engineering applications. Decellularization was performed with the treatment of detergent-like solution. The degree of residual cell content was evaluated by DNA and protein quantification as well as immunostaining. Chemical and mechanical properties were tested for both native and decellularized leek samples in order to investigate the effect of decellularization process on the structure. Swelling, degradation and protein adsorption behavior of decellularized leek samples were also studied. SH-SY5Y human neuroblastoma cell line was used for mammalian cell culture studies. Prior to cell seeding, decellularized leek samples were modified with 3-aminopropyltriethoxysilane (APTES), octadecyltrichlorosilane (OTS) and coated with graphene oxide (GO) in order to enhance cell adhesion. MTT cell viability assay and SEM imaging were performed to observe the cell attachment and proliferation. Prepared decellularized leek tissues are expected to be candidate cellulose based scaffolds for tissue engineering applications both *in vitro* and *in vivo* conditions in future studies.

Keywords: Decellularization, Plants, Cellulose, 3D scaffolds, Tissue Engineering

ÖZET

SELÜLOZ BAZLI POTANSİYEL BİR BİYOMALZEME OLAN PIRASANIN HÜCRESİZLEŞTİRİLMESİ VE KARAKTERİZASYONU

Doku mühendisliğinin temel amacı; zarar görmüş dokuları, hücre yaşamına ortam sağlayan 3 boyutlu doku iskeleleri kullanarak yenilemektir. Şu anda kullanılan doku iskeleleri, insan donörlerden ya da hayvan ürünlerinden elde edilmektedir fakat ihtiyacı karşılayamamaktadır. Son zamanlarda, doğada kolayca bulunabilen biyomalzemeler olan selüloz bazlı doku iskelelerinin, doku mühendisliğindeki uygulamaları bulunmaktadır. Bu çalışmalar, bitki bazlı doku iskelelerinin yara iyileştirme, kalp ve sinir doku mühendisliği gibi birçok farklı uygulamada kullanılabilecek potansiyel bi-yomalzemeler olduğunu göstermektedir. Bu tezde, hücresizleştirme için morfolojik yapısından dolayı (birbirine bağlı, uzun kanal gibi yapılar) pırasa bitkisi seçilmiştir. Pırasa, deterjan bazlı solüsyonla hücresizleştirilmiştir. Hücresizleştirme derecesi, DNA ve protein ölçümleriyle ve hücre çekirdeği boyamasıyla değerlendirilmiştir. Kimyasal ve mekanik özellikler, hücresizleştirme işleminin yapıyı değiştirip değiştirmediğini görebilmek için hücresizleştirmeden önce ve sonra gerçekleştirilmiştir. Pırasa örneklerinin şişme, protein adsorpsiyonu ve bozunma özellikleri de incelenmiştir. SH-SY5Y insan nöroblastoma hücreleri, hücre kültürü deneylerinde kullanılmıştır. Hücre tutunmasını arttırmak için örnekler 3-aminopropiletoksisilan (APTES), oktadesiltriklorosilan (OTS) ve grafen oksit (GO) ile kaplanmıştır. Hücrelerin örneklere tutunması ve çoğalmaları MTT hücre canlılık deneyi ve Taramalı Elektron Mikroskobu görüntüleriyle incelenmiştir. Hazırlanan hücresizleştirilmiş pırasa örneklerinin, ileriki selüloz temelli doku mühendisliği çalışmaları için potansiyel doku iskelesi adayı olması beklenmektedir.

Anahtar Sözcükler: Hücresizleştirme, Bitki, Selüloz, 3B Doku İskeleleri, Doku Mühendisliği

TABLE OF CONTENTS

ACKNOWLEDGMENTS . . . iii
ACADEMIC ETHICS AND INTEGRITY STATEMENT . . . iv
ABSTRACT . . . v
ÖZET . . . vi
LIST OF FIGURES . . . x
LIST OF TABLES . . . xii
LIST OF SYMBOLS . . . xiii
LIST OF ABBREVIATIONS . . . xiv
1. INTRODUCTION . . . 1
1.1 Motivation . . . 1
1.2 Objective . . . 2
1.3 Outline . . . 3
2. BACKGROUND . . . 4
2.1 Scaffolds in Tissue Engineering . . . 4
2.1.1 Synthetic or Natural Biomaterials as Scaffolds . . . 4
2.1.2 Tissue and Organ Transplantations . . . 5
2.2 Decellularization . . . 5
2.2.1 Decellularization Protocols . . . 6
2.2.2 Recellularization . . . 7
2.3 Plants as Potential Scaffolds . . . 9
3. MATERIALS AND METHODS . . . 12
3.1 Pre-Treatment and Decellularization . . . 12
3.2 Evaluation of Decellularization . . . 13
3.2.1 Surface Morphology . . . 13
3.2.1.1 Scanning Electron Microscopy (SEM) . . . 13
3.2.1.2 Profilometer Analysis . . . 14
3.2.2 Immunofluorescence Staining . . . 14
3.2.3 DNA and Protein Quantification . . . 15
3.3 Modification and Characterization of Leek Scaffolds . . . 15

3.3.1 Surface Modification . . . 15
3.3.2 Protein Adsorption Studies . . . 17
3.3.3 Degradation Behavior . . . 17
3.3.4 Swelling Ratio . . . 17
3.3.5 Chemical Analysis . . . 18
3.3.6 Mechanical Properties . . . 18
3.4 Cell Studies . . . 18
3.4.1 MTT Cell Viability Assay . . . 19
3.4.2 Cell Morphology . . . 19
3.5 Statistical Analysis . . . 20
4. RESULTS . . . 21
4.1 Pre-treatment and Decellularization . . . 21
4.2 Evaluation of Decellularization . . . 21
4.2.1 Surface Morphology . . . 21
4.2.1.1 Scanning Electron Micrsocopy (SEM) . . . 21
4.2.1.2 Profilometer Analysis . . . 22
4.2.2 Immunofluorescence Staining . . . 23
4.2.3 DNA and Protein Quantification . . . 24
4.3 Modification and Characterization of Leek Scaffolds . . . 26
4.3.1 Protein Adsoprtion Studies . . . 26
4.3.2 Degradation Behavior . . . 26
4.3.3 Swelling Ratio . . . 27
4.3.4 Chemical Analysis . . . 29
4.3.5 Mechanical Properties . . . 31
4.4 Cell Studies . . . 31
4.4.1 MTT Cell Viability Assay . . . 31
4.4.2 Cell Morphology . . . 32
5. DISCUSSION . . . 34
5.1 Decellularization and Characterization of Leek Scaffolds . . . 34
5.2 Cell Culture Studies . . . 39
5.3 Conclusion . . . 40
5.4 Future Studies . . . 40

APPENDIX A. SUPPORTING INFORMATION 42
A.1 Bradford Protein Quantification Assay 42
REFERENCES 43

LIST OF FIGURES

Figure 2.1	Various bioengineered organs. (a) Ear-shape biodegradable scaffold from PGA. (b) Scaffold implanted on the back of mouse. (c) First human trachea transplant. (d) Artificial bladder. (e) Artificial kidney. (f) Artificial heart-valve	7
Figure 2.2	Tissue decellularization and recellularization concepts.	8
Figure 2.3	Mimicry of animal (rat heart) and plant (Buddleja davidii leaf) vascular structure	9
Figure 3.1	Schematic representation of leek decellularization process; modification with APTES, OTS and GO coating and cell culture with SH-SY5Y human neuroblastoma cells.	13
Figure 3.2	Schematic representation of APTES, OTS modification and GO coating on decellularized leek samples.	16
Figure 4.1	Leek samples at day 0, 1 and 5 of decellularization process.	21
Figure 4.2	SEM images and pattern width histograms of native and decellularized leek samples. SEM images of native leek inner side 2000x (A), 500x (B), pattern width (C); native leek outer side 2000x (D), 500x (E), pattern width (F); decellularized leek inner side 2000x (G), 500x (H), pattern width (I); decellularized leek outer side 2000x (J), 500x (K), pattern width (L).	22
Figure 4.3	Profiles of A. Native inner side B. Native outer side C. Decellularized inner side D. Decellularized outer side of leek samples obtained with the optical profilometer.	23
Figure 4.4	DAPI staining images of leek samples before and after decellularization. A. Day 0, B. Day 1, C. Day 5.	24
Figure 4.5	DNA content was quantified before and after decellularization (n=5).	25
Figure 4.6	Protein content was quantified by Bradford assay before and after decellularization (n=5).	25

Figure 4.7 Protein adsorption capacity of decellularized leek tissues. Human serum albumin was used as protein solution and leeks were interacted with it for 48 hours. (n=3) 26

Figure 4.8 Degradation behavior of decellularized leek samples was observed in PBS at pH=7 and 37°C. 27

Figure 4.9 Swelling ratios of A. Native and decellularized B. APTES, OTS and GO-modified leek samples in PBS and DMEM at room temperature. 28

Figure 4.10 FT-IR analysis of A. inner and outer surfaces of native and decellularized B. APTES, OTS modified and GO-coated leek samples. 30

Figure 4.11 MTT cell viability test results for seeded SH-SY5Y cells on both inner and outer surfaces of decellularized leek and APTES, OTS modified and GO-coated decellularized leek samples at day 1,4 and 7 (n=3). (* $p<0.05$, ** $p<0.01$) 32

Figure 4.12 SEM images of SH-SY5Y cells seeded decellularized leek samples; inner surface (A-B), outer surface (C-D), APTES-coated surface (E-F), OTS-coated surface (G-H), GO-coated surface (I-J). 33

Figure A.1 Calibration curve for Bradford protein quantification assay. 42

LIST OF TABLES

Table 4.1 Mechanical properties of native, decellularized and modified leek samples. 31

LIST OF SYMBOLS

Au	Gold
C	Carbon
$CaCl_2$	Calcium chloride
CH_3	Methyl
CO_2	Carbon dioxide
COOH	Carboxyl
NaCl	Sodium chloride
NaOH	Sodium Hydroxide
NH_2	Amino
O	Oxygen
OH	Hydroxyl
Si	Silicon

LIST OF ABBREVIATIONS

APTES	(3-Aminopropyl)triethoxysilane
BSA	Bovine serum albumin
CHAPS	3-[(3-cholamidopropyl)dimethylammonio]-1-propanesulfonate
DAPI	4,6-diamidino-2-phenylindole
DMEM	Dulbecco's Modified Eagle Medium
DMSO	Dimethyl sulfoxide
ECM	Extracellular Matrix
EDTA	Ethylenediaminetetraacetic acid
ESC	Embryonic stem cells
FBS	Fetal Bovine Serum
FT-IR	Fourier Transform Infrared
GAG	Glyco amino glycans
GO	Graphene oxide
hDFs	Human dermal fibroblasts
HMDS	Hexamethyldisilazane
hPS-CM	Human pluripotent stem cell-derived cardiomyocytes
HSA	Human serum albumin
HUVEC	Human umbilical vein endothelial cells
iPSC	Inducible pluripotent cells
MSCs	Mesenchymal stem cells
MTT	Thiazolyl blue tetrazolium bromide
OTS	Octadecyltrichlorosilane
PDMS	Polydimethylsiloxane
PGA	Poly-glycolic acid
PLA	Poly-lactic acid
PBS	Phosphate Buffer Solution
RGD	Arginine-Glycine-Aspartate
RT	Room temperature

SDS	Sodium Dodecyl Sulfate
SEM	Scanning Electron Microscopy
STE	Sodium chloride Tris-EDTA
UV	Ultraviolet

1. INTRODUCTION

1.1 Motivation

Tissue engineering aims to regenerate damaged tissues or organs by replacing them with biomaterials that provide 3D scaffolds mimicking the *in vivo* cellular microenvironment [1]. There exists many complications with synthetically produced biomaterials that are used for tissue repairing in terms of biocompatibility, biodegradability, scaffold architecture, mechanical properties and vascularization [2]. Natural source of tissue or organ transplantation is human donors or animal products however the need exceeds the availability. In 2018, there were 113,759 patients in waiting list in United States and only 17,554 donors were found, 36,529 organs were transplanted [3]. Additionally, allografts and xenografts have the risk of rejection and autografts are painful conditions for patients. All of these methods are costly and cause challenges to access convenient donors [2]. Decellularization is a novel approach for obtaining a 3D organ-derived scaffold materials that are formed from extracellular matrix (ECM) which provides biomechanical support and a microenvironment for cell attachment and proliferation [4]. The main aim of decellularization protocol is removal of cellular content with exposure of the tissue to ionic detergent-like solutions without disrupting the biochemical composition and structural integrity [5]. Because of the insufficiency of human donors and animal products; recently, plant-derived cellulose-based scaffolds have been investigated. Plants are easily available in nature and cost effective compared to animal products. In addition, the similarities between plant and animal tissues makes these scaffolds a good alternative for tissue engineering applications [6]. Cellulose is the most abundant biopolymer in nature and due to its biocompatibility, biodegradability and hydrophilicity; it has been used in different applications such as wound dressing, tissue engineering, drug delivery etc. Also it has antimicrobial properties which facilitate recovery process and shows no toxic effects [7]. There are several hydroxyl groups on cellulose that ease the functionalization of the surface leading to controllable and adjustable mechanical properties [8]. In the literature; the first example of plant de-

cellularization was apple tissue which was examined both and *in vivo* studies by D.J. Modulevsky et al. [1],[9]. Another promising study was spinach decellularization in which J.R. Gershlak et al investigated the vascularization issues [6]. In addition, a different group observed decellularization and functionalization of a variety of plants such as bamboo, vanilla, orchid etc., on mammalian cell culture [10]. Their results showed that cellulose-based scaffolds were potential candidates for tissue engineering applications. In this thesis, leek was decellularized and its material properties were characterized. SHSY-5Y human neruoblastoma cells was used in order to evaluate the potential of this plant based cellulosic scaffold for future applications due to its morphological structure. Cell adhesion and viability on decellularized leek samples were observed in order to investigate the leek tissue as a potential tissue engineering scaffold.

1.2 Objective

In this thesis, leek was chosen for the resemblance between its topographical aspects, which were elongated and interconnected channel-like patterns for possible tissue engineering applications. Leek tissues were decellularized with detergent-like solutions in order to remove plant cell content and keep the remaining ECM-based scaffold. Objectives of this study were:

- Decellularization of leek tissues
- Evaluation of decellularization with immunostaining, DNA and protein quantifications
- Comparison of chemical, mechanical and morphological properties of native and decellularized leek samples
- Mammalian cell culture with SH-SY5Y human neuroblastoma cell line
- Investigation of cell adhesion and viability on these cellulose-based scaffolds

The main aim of this study is to demonstrate that leek-derived cellulose-based scaffolds supported *in vitro* mammalian cell culture, which indicate that plant decellularization may be a promising alternative scaffolds for potential tissue engineering applications.

1.3 Outline

This thesis is presented as follows:

Background information about tissue engineering scaffolds and decellularization of animal and plant tissues is explained in chapter 2. In chapter 3, experimental methods are described. Results are presented in chapter 4 and discussion of results are given in chapter 5.

2. BACKGROUND

2.1 Scaffolds in Tissue Engineering

Tissue engineering is an interdisciplinary area that mainly aims to regenerate the damaged tissue by using biomaterial-derived 3D porous scaffolds which act as a template for cells in order to repair and improve the functionality of injured tissue or form totally a new one [11]. These scaffolds can be prepared either cell-seeded *in vitro* or directly implanted to a patient without cell culture and they are supported with growth factors for providing mechanical or chemical stimuli in order to enhance cell adhesion and migration [2]. Scaffolds should mimic the native extracellular matrix (ECM) properties therefore some requirements are needed for material choice. The first criterion is biocompatibility otherwise severe inflammatory reactions may occur and the body rejects the scaffold. Secondly, the scaffolds material should be biodegradable in order to allow native cells to adhere before any chronical immune response come into existence. However, there should be enough time prior to degradation for cells to form their own cellular environment also; the by-products of degradation should be non-toxic and easily removable from the human body. Mechanical stability is another essential prerequisite for scaffold for implementing the structural integrity at the anatomical site. In addition, porous structure is necessary for nutrients and gas transport for cells to form their own ECM though, pore sizes should be optimal as not compromising with the mechanical stability [2],[12].

2.1.1 Synthetic or Natural Biomaterials as Scaffolds

Polymers, bioceramics and hybrid materials either natural or human-made are generally used as biomaterials for biomedical applications. Natural polymers like hyaluronic acid, collagen and chitosan show high biocompatibility and low immunogenicity however; their low mechanical stability and not adjustable degradation rates

are downsides [13]. Synthetic materials like Poly-glycolic acid (PGA) and Poly-lactic acid (PLA) are more advantageous than natural ones in terms of porosity, degradation and mechanical properties that are tailored for specific applications. Also, they are cheaper than biological ones and can be produced in high quantities uniformly with a long shelf-life [14]. Beside these advantages, the major limitation of synthetic materials is the lack of biological constituents of ECM. In addition, their degradation by-products may be toxic effects on human body. Even though, these biomaterials are currently used products in medical industry, there are still several drawbacks as described above [15].

2.1.2 Tissue and Organ Transplantations

Another treatment approach is using autografts and allografts for replacing the damaged tissue. Using patient's own tissues from a different part of his/her own body is autografting. This method provides a gold standard treatment without any immune reaction however, only limited number of autografts are available. Allografts are taken from somebody else's body and their rejection rate due to pathogen transmission and infection higher than autografts [16]. Organ transplantation is the greatest achievement in medicine; receiving a new organ increases the patient's life quality while decreasing the rate of morbidity and mortality for patients who suffer from organ failure. However, main constrict of organ transplantation is the increasing number of patients that are available on donor waiting list [17]. Because of the increasing mortality rate due to organ shortage, different methods such as decellularization of animal and plants tissues for various tissue engineering applications are still developing.

2.2 Decellularization

Decellularization process mainly aims the removal of native cells and genetic material while retaining the 3D structure and mechanical integrity. The remaining ECM provides a scaffold for patient's own cells to form a personalized new tissue.

Up to now, this method has been successfully used for creating different types of tissues and organs such as blood vessel, heart valve, cornea, trachea, urinary bladder, kidney, liver, lung and esophagus [18]. The superior property of decellularized tissues than other biomaterials that are used as scaffolds is the contribution of ECM proteins to enhance cell mitogenesis and chemotaxis. Cell differentiation and proliferation is induced by these biological elements and augment the repairing phase [19].

2.2.1 Decellularization Protocols

Several protocols are currently used for decellularization which are mainly categorized as physical, chemical and enzymatic and chosen in compliance with the tissue type. Physical methods include freezing, direct pressure, sonication or mechanical agitation that disrupt cellular membranes and cell lysis by causing sudden changes in tissue's physical conditions. Chemical methods that are used for decellularization are diversified such as treatments in acidic and alkaline environments, ionic and non-ionic detergent-like solutions, hypotonic or hypertonic media. Acidic or basic solutions can effectively disrupt cell membranes and organelles for removing the genetic material however they also harm some of the ECM proteins. Non-ionic detergents can be used for breaking lipid-lipid and lipid-protein interactions in the cellular environment however they don't show any effect on protein-protein interactions which can cause remaining of nuclear material. On the other hand, ionic detergents disrupt protein-protein interactions in order to solubilize cytoplasm for removing cellular content but they can also cause denaturing of membrane proteins that are found in ECM [20]. Mostly studied non-ionic detergent for decellularization is Trition-X-100 and ionic one is SDS (Sodium Dodecyl Sulfate). These chemicals can be used alone or in combination according to strength of the organ. Nonetheless, optimal decellularization method should be tailored for each specific applications [21]. Zwitterionic detergents show the properties of both non-ionic and ionic detergents and most commonly used one is 3-[(3-cholamidopropyl)dimethylammonio]-1-propanesulfonate (CHAPS) which has been especially studied for decellularization of blood vessels [20],[22]. Hypertonic and hypotonic solutions cause lysis of native cells by osmotic shock however they have also

disruptive effect on glyco amino glycans (GAG) of ECM [20],[23]. Enzymatic methods are also used for decellularization and most studied one is Trypsin/EDTA. Despite it reduces cellular content efficiently, increasing exposure time of Trypsin/EDTA induces loss of ECM proteins and structural integrity [24].



Figure 2.1 Various bioengineered organs. (a) Ear-shape biodegradable scaffold from PGA. (b) Scaffold implanted on the back of mouse. (c) First human trachea transplant. (d) Artificial bladder. (e) Artificial kidney. (f) Artificial heart-valve [25].

2.2.2 Recellularization

3D ECM-derived engineered tissues and organs require to create new parenchyma, vasculature and underlying supporting structures. The optimal way to reach this goal is recellularization of the tissue by using easily proliferative and self-renewable cell sources. These cells may be obtained from patient's own cells (autologous) that eliminate the rejection possibility and decrease immune response also immunosuppressive drug usage. Most challenging issue with autologous cells is that they cannot be easily

harvested from most organs like pancreas, lung and heart and their numbers are generally insufficient for nascent tissue. On the other hand, allogenic cells can be harvested from younger and healthier individuals in larger amounts. Allogenic cells are more advantageous than autologous ones because they can be isolated, multiplied and characterized before seeding also modified *in vitro* with genes if necessary [4]. Xenogenic cells from animals can be alternative source for recellularization however, severe immunological reactions may occur [26]. Stem and progenitor cells such as embryonic stem cells (ESC), fetal cells, umbilical cord blood-derived cells and adult-derived inducible pluripotent cells (iPSCs) are mostly used for various tissue engineering applications. Parenchymal and supportive cells like fibroblasts are obtained from the organ of interest via biopsy [4].

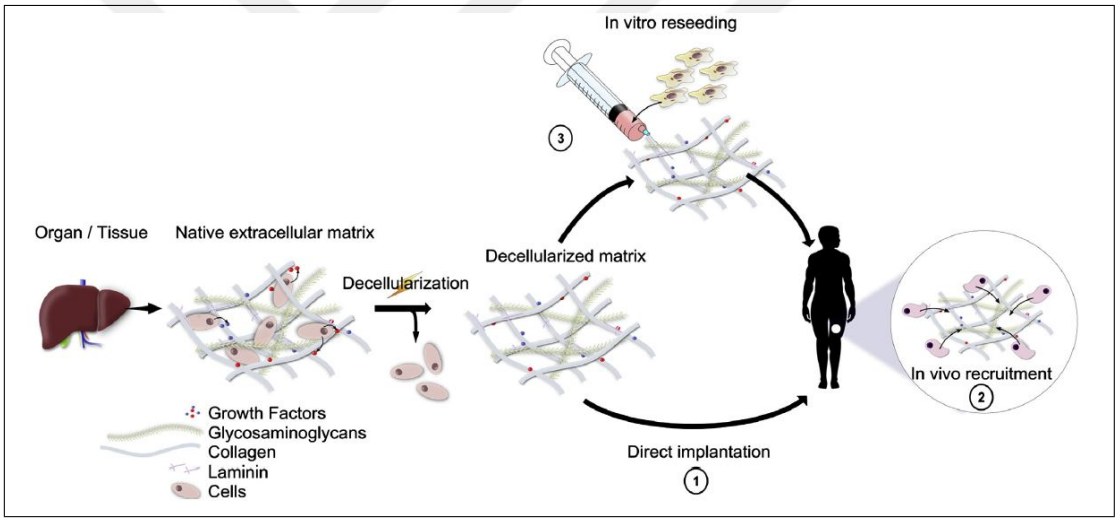


Figure 2.2 Tissue decellularization and recellularization concepts. [27].

Decellularized scaffolds can either directly implanted to the patient and her/his own cells are expected to attach and proliferate on them or they can be seeded with cells prior to implantation in order to guide patient's cells for multiplying while gaining the specific function [26]. Cells can be directly injected through the parenchymal tissue, infused step by step or perfused continuously for delivering into decellularized scaffolds. Seeding efficiency might decrease due to the directly injected cells and continuous perfusion may cause less cell-matrix attachment due to persistent flow. The optimal method is multistep infusion for homogenous cell culture [28].

2.3 Plants as Potential Scaffolds

Decellularization of mammalian tissues is an effective method for repairing damaged tissues and organs with higher biocompatibility because of ECM structure and contents by decreasing the immunogenicity. However, available mammalian tissues are still insufficient to meet the need. Therefore; readily available, cost-effective alternative sources for decellularization are required. Mimicry of plant and animal vascular network structures makes plants potential candidates for decellularization-based scaffolds [6].

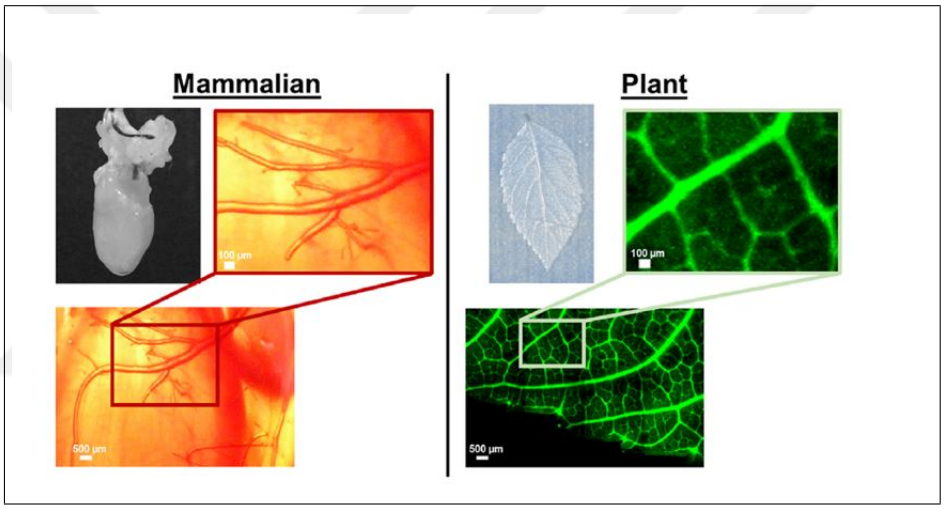


Figure 2.3 Mimicry of animal (rat heart) and plant (Buddleja davidii leaf) vascular structure [6].

After a plant is decellularized, the cell wall that is mainly formed from cellulose and surrounds the plant cells is remained. The cell wall of a plant gives the shape of plant organs and connects adjoining cells into tissues. Similar to ECM of animal cells, cell wall controls growth and proliferation of cells. The strength of the cell wall is related to cellulose microfibrils that are formed from extensively cross-linked hemicellulose polysaccharide chains. Each microfibril consists of glucose residues that are linked together by β (1$\rightarrow$4) glycosidic bonds into a straight glucan chain [29]. Cellulose is one of the most abundant biodegradable material that is easily accessible in nature and due to its biocompatibility, hydrophilicity, nontoxicity and antimicrobial properties; it is used for various biomedical and tissue engineering applications. Wound dressing, controlled drug delivery and purification of blood are some examples of these

applications [7]. Numerous hydrogen bonds and low intermolecular attractive forces of cellulose polymers provide strength and flexible structure. Therefore, decellularized plant-derived cellulose based biomaterials can support human cell attachment and proliferation [10]. In the literature; the first example of decellularized plant derived scaffold that is investigated by D.J. Modulevsky et al. is apple tissue. They decellularized the apple tissue with 0.5% SDS for 12 hours then characterized the obtained scaffolds by functionalizing with collagen or glutaraldehyde crosslinking in order to enhance mammalian cell attachment. For cell culture experiments, they used three different cell lines C2C12 mouse myoblasts, NIH3T3 mouse fibroblasts and HeLa human cervical carcinoma cells. Immunofluorescence staining methods was used for determining the decellularization degree also morphological and mechanical analysis were done. Their results showed that different surface modifications didn't significantly affect the cell behavior besides, viability and proliferation of different cell types were similar. This study demonstrated that cellulose scaffolds are potential candidates for 3D mammalian cell culture [9]. Same research group was further investigated biocompatibility of decellularized apple tissue *in vivo*. Scaffolds were subcutaneously implanted in 6-9 weeks old male and female mice. Their results demonstrated that by 8 weeks post-implantation the decellularized apple-derived scaffold has been accepted by the host animal. In addition, they promoted cell proliferation, ECM deposition and vascularization also showed low inflammatory response [1]. Following these studies, J.R. Gershlak et al. decellularized spinach leaves by using the biomimetics between vasculature of a mammalian's heart and a plant's leaf. Spinach leaves were treated with 10% SDS for 5 days by perfusion of the solution through cannulas. Human umbilical vein endothelial cells (HUVEC) and human pluripotent stem cell-derived cardiomyocytes (hPS-CM) were used for recellularization after scaffolds were coated with fibronectin. In addition to human cell culture, contraction properties of this scaffolds were also examined. In spite of their results were promising, further investigations are needed in order to determine whether decellularized plants are convenient for clinical applications [6]. G. Fontana et al. observed decellularization of various plants such as bamboo, orchid, vanilla, parsley, calathea, anthurium and solenostemon using SDS, Triton-x-100 and bleach in combination for total treatment of 7 days. Prior to cell seeding, scaffold surface was functionalized with mineralization and RGD-dopamine conjugate then human dermal

fibroblasts (hDFs) and mesenchymal stem cells (MSCs) were used for cell culture. According to their results, biofunctionalization of decellularized plant tissue can enhance human cell adhesion. In addition, human cells migrate in accordance with topographical features of plant tissue by conforming to structural motifs or aligning cell patterns [10].

3. MATERIALS AND METHODS

3.1 Pre-Treatment and Decellularization

Leek samples were obtained from a local grocery store and were stored at -20°C until use. First, leek tissues were sliced and cut layer by layer. Then, samples were washed with deionized water (dH_2O) under vacuum for 3 hours and were kept at -80°C overnight. Leek tissues were then decellularized (as seen in Figure 3.1.) with 1.0% Sodium Dodecyl Sulfate (SDS) (Sigma) treatment at 37°C for 5 days in order to obtain a 3-D structure by removing the cellular content [6],[9]. Then, samples were washed several times with dH_2O followed by Phosphate Buffer Solution (PBS) until residual SDS was completely washed out. Afterwards samples were placed in absolute ethanol solution at 65°C for maximum 24 hours for chlorophyll removal [30]. Following this step, decellularized scaffolds were washed with PBS twice and kept in PBS at 37°C overnight in order to remove excess ethanol. Decellularized leek samples were then stored at +4°C for further use.

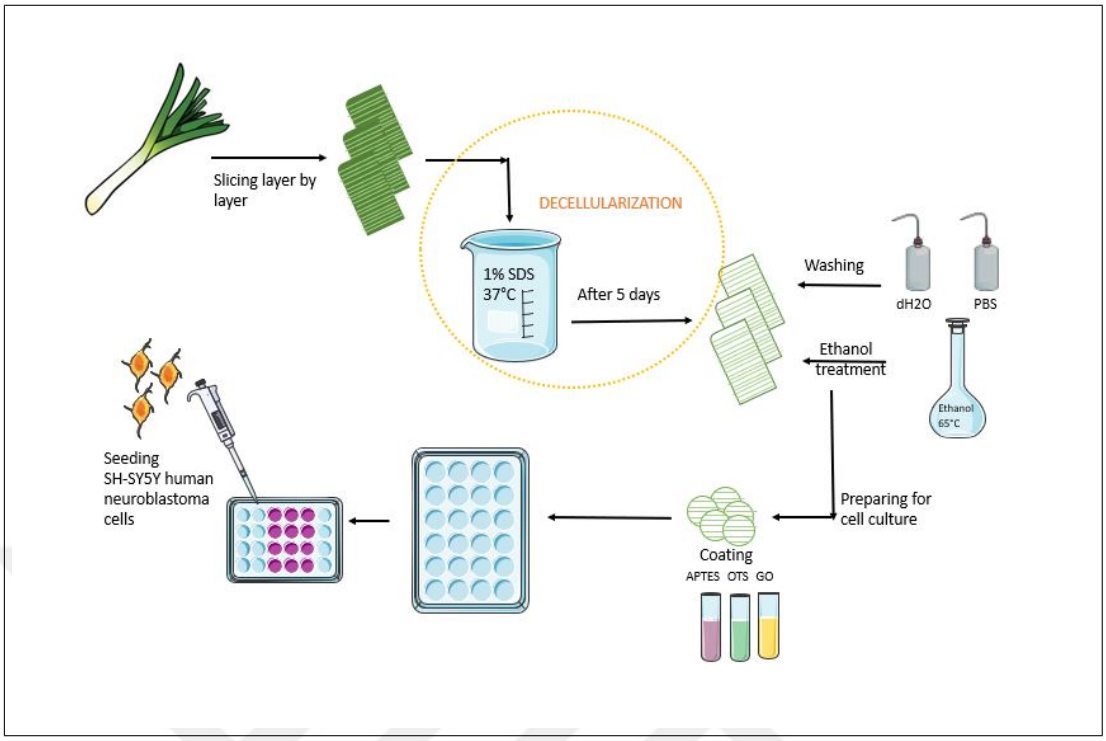


Figure 3.1 Schematic representation of leek decellularization process; modification with APTES, OTS and GO coating and cell culture with SH-SY5Y human neuroblastoma cells.

3.2 Evaluation of Decellularization

3.2.1 Surface Morphology

3.2.1.1 Scanning Electron Microscopy (SEM). Surface Morphology was investigated with SEM (FEI-Philips XL30) to observe morphological difference between native and decellularized samples. At first samples were fixed with 4.0 % formaldehyde containing fixative solution for overnight [31]. In order to remove the formaldehyde, samples were washed with fresh PBS three times. Secondly, samples were dehyrdated by immersion in a series of ethanol solution of 30%, 50%, 80% and 95% respectively for 15 minutes each. Finally, Hexamethyldisilazane (HMDS) (Sigma) was dropped on the samples and they were placed in desiccator under vacuum for 10 minutes. Excess HMDS was removed and samples were left to dry overnight. Prior to imaging in SEM, samples were coated 50 nm Au by sputter coating (Polaron SC 7640 Sputter Coater) [6].

3.2.1.2 Profilometer Analysis. Profilometer analysis was performed with interference -based Optical Profilometer (Zygo NewView 7200) for native and decellularized leek samples in order to measure pattern depths . Measurement sample was placed on the stepper-motor controlled XY stage and centered. Piezo-controlled interferometric lens head (5X Nikon CF-IC Epi Plan TI interferometry objective lens) was adjusted in z-axis to generate the focused surface image and interference pattern, simultaneously. Created interference patterns were captured by a video camera. Then, intensity level at each camera pixel was processed with the software (MetroPro) to generate the height map of the test surface.

3.2.2 Immunofluorescence Staining

Immunohistochemistry was performed in order to evaluate degree of decellularization. Leek samples were first fixed with 4.0 % formaldehyde (Sigma) fixation solution in PBS and pH was adjusted to 7.0 with 1N NaOH. After the solution was cooled and filtered; it was used for the fixation solution preparation. 0.1% Triton-X-100 (Sigma), 1.0% glutaraldehyde (Sigma), 2mM $CaCl_2$ (Sigma) and 1.0% (w/v) sucrose was added to the solution and kept on ice until use. Samples were incubated in the fixative solution overnight. Samples were washed with PBS three times to remove formaldehyde from tissues. Samples were then placed in 0.1% Triton-X-100 (Sigma) solution for one hour at RT [31]. After the fixation step, DAPI (4,6-diamidino-2-phenylindole) (Life Technologies) staining was applied to observe if the nuclei remained or not following the decellularization process. DAPI dye was dissolved in methanol and 2.1 μL of methanolic stock solution was diluted into 100 μL PBS. Intermediate solution was diluted 1:1000 in PBS to obtain staining solution. Staining solution was added on the cells and kept on a gentle shaker for three minutes. Samples were washed with PBS prior to imaging. Fluorescence microscope (Leica DFC 295) was used for imaging and nuclear stain was visible under violet filter [32].

3.2.3 DNA and Protein Quantification

Both native and decellularized leek samples were analyzed to observe the reduction in the amount of DNA and protein after decellularization process. DNA quantity was measured with a well-established protocol [33]. Briefly, 720 mL STE buffer (100mM Tris (pH=8.5), 5mM EDTA, 0.2% SDS, 200mM NaCl) and 30mL Proteinase K solution (10mg/mL stock solution) (P2308 Sigma-Aldrich Proteinase K from Tritirachium album) was added onto the decellularized samples and incubated at 55°C on heating block for 3 hours by mixing with vortex (Bead Bug Microtube homogenizer, Benchmark scientific) with one hour intervals at top speed for 10 seconds in order to isolate the DNA from tissues. Proteinase K was inactivated at 70°C for 5 minutes then quenched on ice for 5 minutes. After centrifuging for 10 minutes at full speed, the solution was transferred to a new tube containing 720 mL isopropanol by decantation. DNA was precipitated by inverting the tube and spun down for 5 minutes at full speed. After supernatant was removed, the pellet was washed with 70% ethanol. DNA was spun down for 5 minutes at full speed again and supernatant was removed. DNA was left to dry for 1-2 minutes then resuspended at 55°C for 1 hour. Quantitative result was obtained from DNA content reading by spectrophotometer (Nanodrop 2000c Spectrophotometer, Thermo Scientific). Protein quantification was done with Bradford Assay Kit [34]. The Coomassie brilliant blue dye was used to determine protein concentrations and a calibration curve was formed with bovine serum albumin (BSA) (Biosera) as a standard. Absorbance values were read at 590nm and 450nm by using microplate reader (Bio-Rad iMark).

3.3 Modification and Characterization of Leek Scaffolds

3.3.1 Surface Modification

Decellularized leek samples were modified with 3-aminopropyltriethoxysilane (APTES), Octadecyltrichlorosilane (OTS) and coated with Graphene Oxide (GO) in

order to enhance cell attachment and proliferation prior to cell culture experiments [Figure 3.2]. 5.0% (v/v) APTES solution was prepared in dH_2O and pH was adjusted to 4.0 by adding glacial acetic acid (99.5%) under stirring. Solution was poured on the inner sides of samples and kept at RT for 2 hours. Then, samples were cured at 60°C in an oven after washed with dH_2O. Unreacted APTES was removed by washing the samples with ethanol and dH_2O respectively [35]. 1.0% (w/v) OTS solution was prepared in hexane. This solution was dispersed on decellularized leek samples for 30 seconds. In order to remove excess OTS, samples were washed with fresh hexane (×2), ethanol (×2) and dH_2O (×2). Samples were exposed to N_2 and annealed at 60°C for 1 hour [36]. 0.5mg/mL GO solution was prepared in dH_2O and homogenized with ultrasonic homogenizer in an ice bath for 1 hour. Prior to coating decellularized leek samples were treated with UV-Ozone for 4 minutes in order to activate the surface. GO solution was added onto the samples and kept at +4°C overnight. GO solution was removed and samples were washed with PBS twice [37].

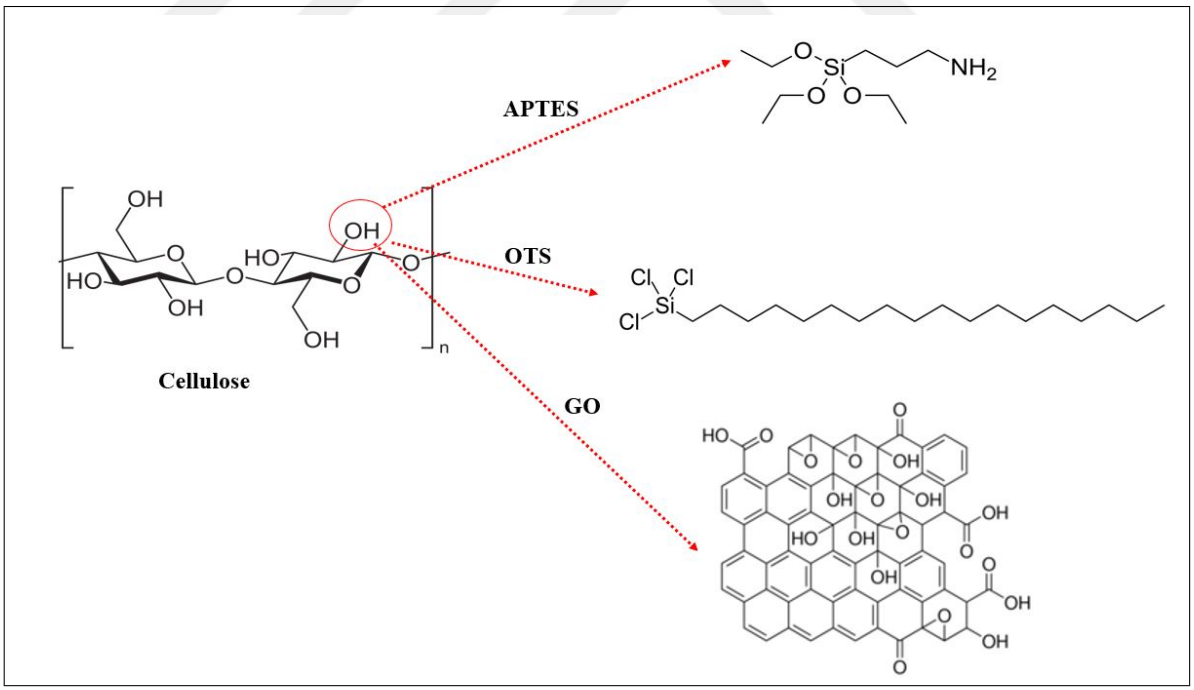


Figure 3.2 Schematic representation of APTES, OTS modification and GO coating on decellularized leek samples.

3.3.2 Protein Adsorption Studies

In order to measure protein adsorption capacity of decellularized leek samples, 1.0% (w/v) protein solution was prepared with human serum albumin (HSA) (Sigma) in PBS. Initial protein concentration of this solution was measured by using spectrophotometer (Nanodrop 2000c Spectrophotometer, Thermo Scientific). Decellularized leek samples were interacted with this solution and measurements were taken at hourly for the first 6 hours and at 12, 24 and 48 hours. Protein concentration of the solution was measured before and after interacting with decellularized leek samples and the difference between initial and final concentrations showed the adsorbed protein (AP) in terms of miligram protein over gram of leek sample by decellularized leek samples (Eq. 3.1) [38].

$$AP = (C_{\mathrm{I}} - C_{\mathrm{t}})/W_{\mathrm{I}} \tag{3.1}$$

where C_I is the initial protein concentration, C_t is the measured protein concentration after an interaction of t hours and W_I is the initial weight of the leek sample.

3.3.3 Degradation Behavior

Decellularized leek samples were dried at 60°C in an oven overnight and weighed after the water content was removed. Samples were placed in PBS (pH 7.0) at 37°C for mimicking the cellular milieu and weight loss of samples were observed consecutively for 21 days in order to determine the degradation rate [39].

3.3.4 Swelling Ratio

Swelling test was done in order to determine fluid absorption capacity of leek-derived scaffolds. The test was applied both in PBS and DMEM (Dulbecco's Modified Eagle Medium) for 24 hours. Native and decellularized samples were dried at 40°C prior to test. After drying, samples were weighed, and the swelling ratio was determined by

immersing fluids at RT. The sample weights were measured at different time points from 30s to 24h. The swelling ratio (SR) were calculated from the Eq. 3.2:

$$SR(\%) = ((W_t - W_0)x100)/W_0) \tag{3.2}$$

where W_t is the weight of sample after time point t and W_0 is the weight of initial dry sample [40].

3.3.5 Chemical Analysis

Chemical structure of the native and decellularized leek samples were analyzed by FT-IR. Also, chemical analysis of APTES, OTS modified and GO coated leek samples were done in order to characterize the modification and coating on the surface (Perkin Elmer, Spectrum 100). FT-IR device was used for experiments in the range of 4000-400 cm^{-1}.

3.3.6 Mechanical Properties

Native and decellularized samples were tested to observe the effects of decellularization on mechanical properties. Tensile strength and elastic modulus measurements were done with universal testing machine (Lloyd Instruments LF Plus). Sample dimensions were 10 mm/ 0.5 mm (width/thick). Tensile test was performed with following specifications; preload stress (2N), preload speed (21 mm/min), test speed (1 mm/s).

3.4 Cell Studies

Prior to cell seeding, 24-well plates were coated with Polydimethylsiloxane (PDMS) in order to stabilize decellularized leek samples by attaching them on plates. SYLGARD 184 Silicone Elastomer Kit (Dow Corning) was used for preparing PDMS by mixing 20:1 (w/w) silicone elastomer/curing agent. This mixture was placed in

a vacuum chamber for 30-45 minutes for removing air bubbles. Uncured PDMS was poured on wells and decellularized leek samples were placed on PDMS layer. Plates were kept at 60°C in an oven overnight for curing. Sterilization was done by washing samples with 70% ethanol for 15 minutes then exposing to UV light for 45 minutes. Samples were washed with PBS twice.

SH-SY5Y human neuroblastoma cell line (ATCC CRL-2266) was used in this thesis as a model cell line. Cells were cultured in DMEM/F12 (Dulbecco's Modified Eagle Medium: Nutrient Mixture F-12),(Gibco), supplemented with 10% FBS (Fetal Bovine Serum) (Sigma), 1% penicillin/streptomycin (Biosera) at 37°C and 5% CO_2. $37.5x10^3$ cells per well were seeded on decellularized leek samples. Cell culture media was changed every 48 hours for continued cell proliferation [41].

3.4.1 MTT Cell Viability Assay

MTT assay was done in order to measure cell viability on the decellularized scaffolds. 5mg/mL MTT (3-(4,5-Dimethylthiazol-2-yl)-2-5-Diphenyltetrazolium Bromide) stock solution was prepared in PBS and filtered. 10% (v/v) MTT solution was added onto cell-seeded scaffolds and incubated at 37°C for 3 hours. All the medium was removed and 500μL of DMSO was added to each well on the shaker for 5-10 minutes. 100 μL of each well was transferred to the 96-well plate and by using microplate reader (Bio-Rad iMark), absorbance values were read at 570nm and 750nm [42]. The experiment was repeated at day 1, 4 and 7 of cell seeding and viability of cells was determined.

3.4.2 Cell Morphology

SEM analysis was done after cell seeding on decellularized leek samples in order to observe cell adhesion. At day 7 of cell seeding, growth medium was dispensed, and cells were washed with PBS twice. 3% glutaraldehyde solution was prepared in PBS

for fixation of cells. Samples were dispersed in this solution for 30 minutes, then PBS wash was repeated 3 times to remove the glutaraldehyde. Dehydration and imaging steps were done as described previously in Section 3.2.1.1. [6].

3.5 Statistical Analysis

All presented values are the average ± standard deviation. Where applicable, we assessed statistical significance by performing a one-way ANOVA with a Tukey's post-hoc test.

4. RESULTS

4.1 Pre-treatment and Decellularization

Leek tissues were cut as 4 cm trimmed stalks and leek tissue samples were taken from each layer by punchers then decellularized following the established protocol in order to remove cellular content and keep the extracellular matrix of the structure. After 5 days of SDS-treatment, chlorophyll broke down in leek samples entirely and become almost transparent which is a sign of decellularization (Figure 4.1).



Figure 4.1 Leek samples at day 0, 1 and 5 of decellularization process.

4.2 Evaluation of Decellularization

4.2.1 Surface Morphology

4.2.1.1 Scanning Electron Micrsocopy (SEM). According to the SEM images as seen in Figure 4.2; after the decellularization process, there was no significant change in scaffold's topographical structure. While removing the cellular content of leek samples, morphological structure remained intact, which indicated that primary goal was achieved. Measured pattern widths of decellularized leek samples were narrower than native ones according to histogram (Figure 4.2.) however, pattern borders became clearer. Inner side of leek pattern width measured from approximately 23.00±1.50 μm to 17.00±2.09μm after decellularization whereas outer side of leek patterns was larger

than inner side 35.00±2.90μm and 24.00±2.07μm native and decellularized respectively.

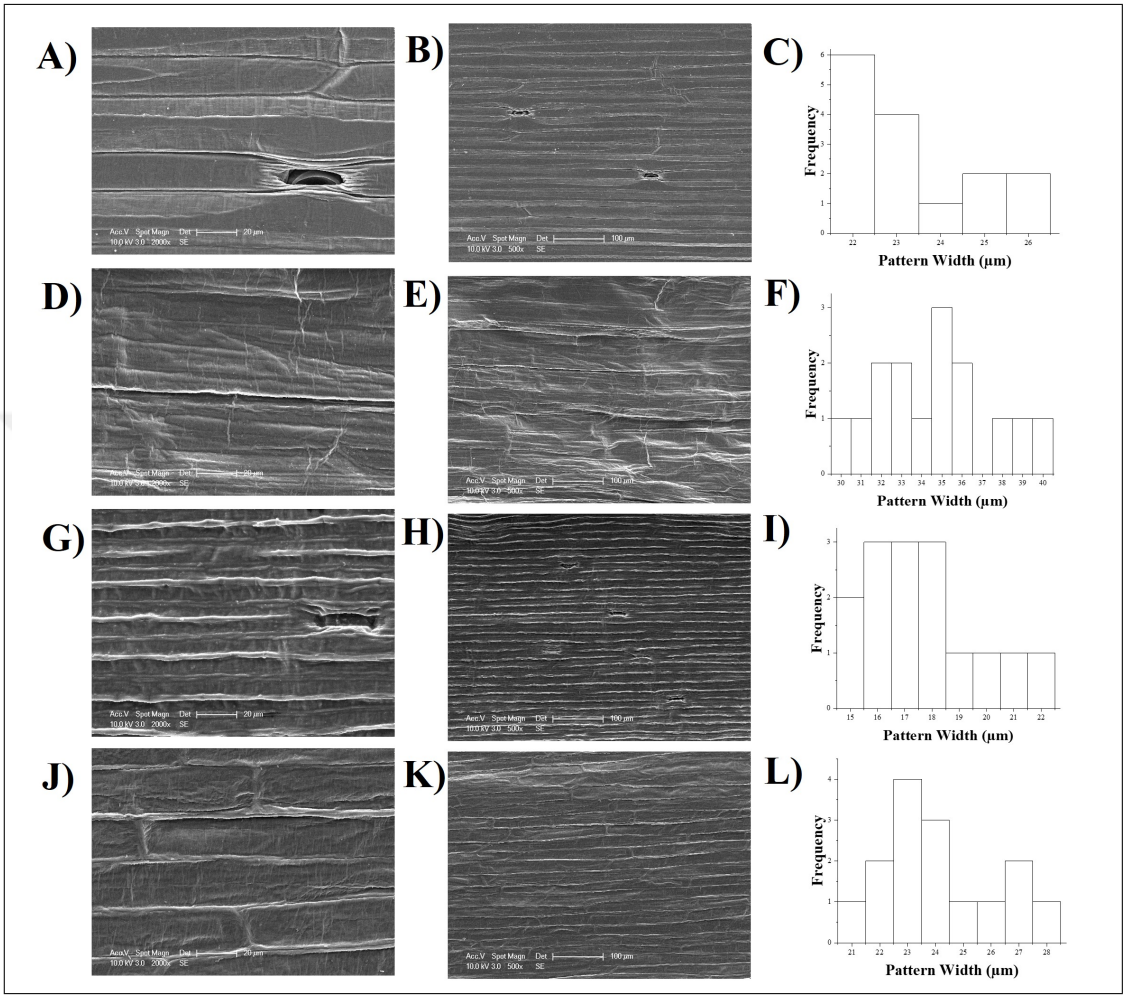


Figure 4.2 SEM images and pattern width histograms of native and decellularized leek samples. SEM images of native leek inner side 2000x (A), 500x (B), pattern width (C); native leek outer side 2000x (D), 500x (E), pattern width (F); decellularized leek inner side 2000x (G), 500x (H), pattern width (I); decellularized leek outer side 2000x (J), 500x (K), pattern width (L).

4.2.1.2 Profilometer Analysis. According to profilometer analysis results (Figure 4.3); the pattern depth of inner and outer surface of native leek was $\sim$ 200 μm and 100 μm respectively. Outer surface of leek tissue was composed of more profound and larger sized patterns. After decellularization; while pattern depth of inner surface was measured to be $\sim$ 300 μm; deepness of outer surface patterns were $\sim$ 50 μm.

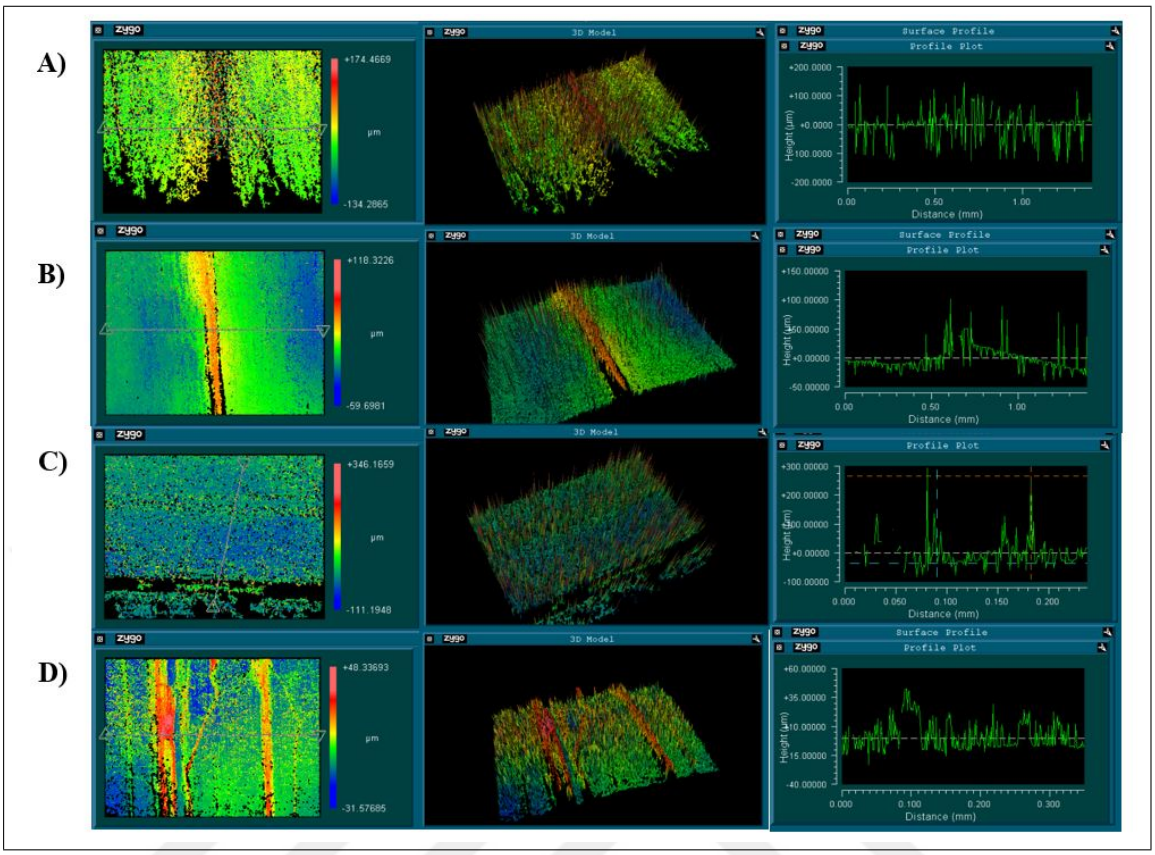


Figure 4.3 Profiles of A. Native inner side B. Native outer side C. Decellularized inner side D. Decellularized outer side of leek samples obtained with the optical profilometer.

4.2.2 Immunofluorescence Staining

In order to evaluate the degree of decellularization by immunohistochemistry; DAPI staining was performed. DAPI solution bound the nucleic acids of cells and nuclei were stained blue under violet light. The experiment was done for native (Day 0) and decellularized (Day 5) samples for the comparison. After 1 day of SDS-treatment, it was observed that nuclei began to deform however, they were still found in the scaffolds. Decellularization procedure was completed after 5 days of SDS-treatment with total nuclei removal as shown in DAPI staining results (Figure 4.4).

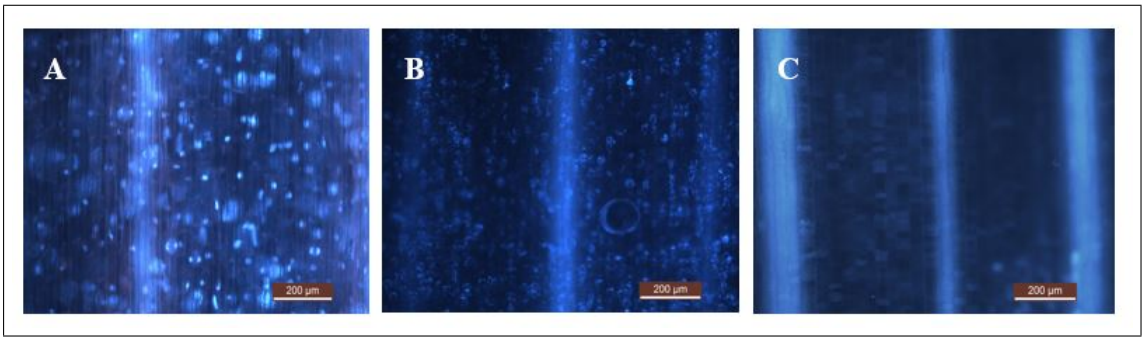


Figure 4.4 DAPI staining images of leek samples before and after decellularization. A. Day 0, B. Day 1, C. Day 5.

4.2.3 DNA and Protein Quantification

DNA and protein quantification were measured to ensure that removal of nuclei and cellular proteins from the decellularized leek scaffolds was successful. According to DNA quantification results (Figure 4.5); after the decellularization process, 83.80% of the total amount of plant DNA was decreased (from 485.83±24.29 to 78.66± 3.93 ng DNA/μL solution) but not completely removed. However, DAPI staining results showed that the nuclei of decellularized (Day 5) leek were completely disposed of. According to Bradford assay (Figure 4.6), at day 5, 90.37 % of the total protein content was removed (from 0.92±0.05 to 0.089±0.0045 ng protein/ mg tissue). Therefore, decellularization protocol, 5 days of SDS treatment was sufficient according to DAPI staining and Bradford assay results.

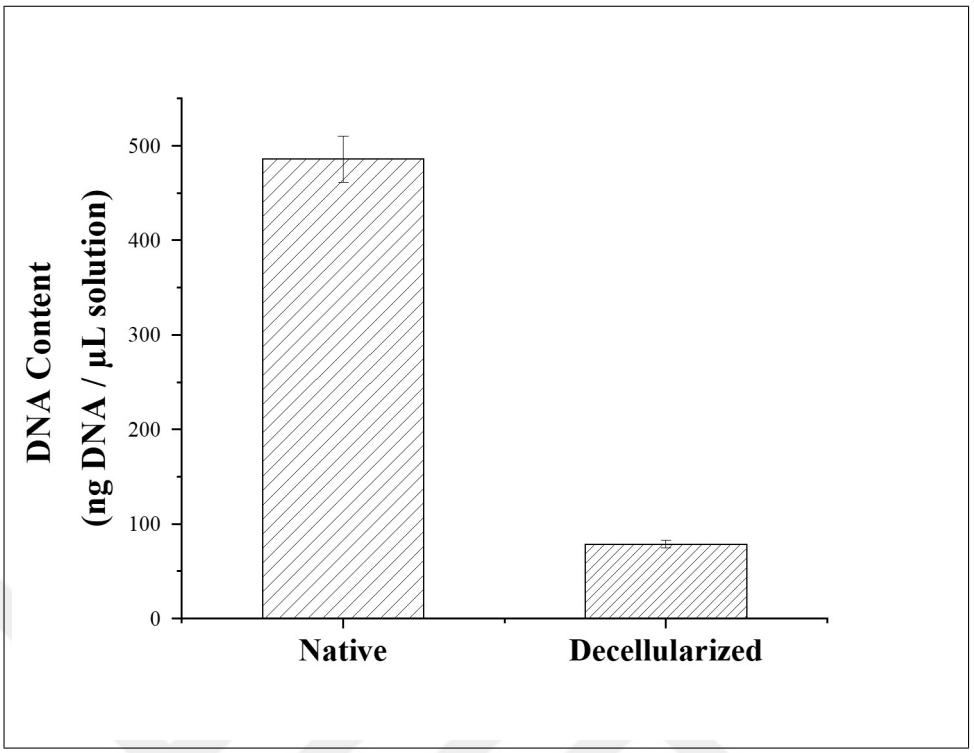


Figure 4.5 DNA content was quantified before and after decellularization (n=5).

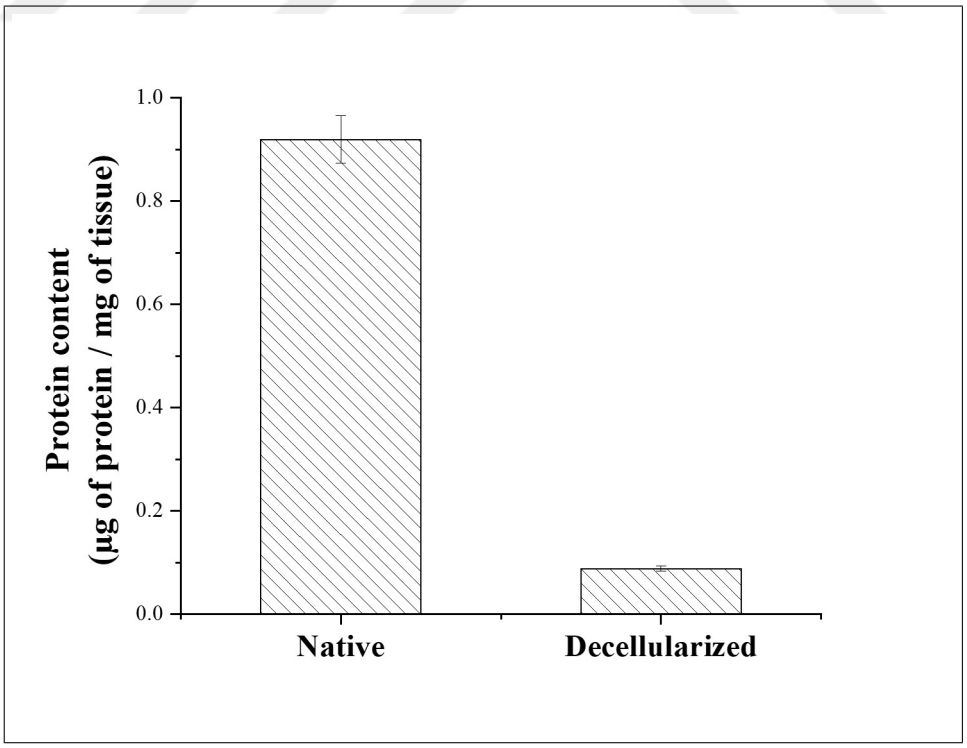


Figure 4.6 Protein content was quantified by Bradford assay before and after decellularization (n=5).

4.3 Modification and Characterization of Leek Scaffolds

4.3.1 Protein Adsoprtion Studies

Leek samples were incubated with HSA solution (5mg/mL) for 48 hours. Between 12-24 hours protein adsorption reached equilibrium and after 24 hours, highest adsorption capacity was measured as 495.68 mg protein/ g leek sample as seen in Figure 4.7. After this point, adsorped protein quantity slightly decreased due to saturation related to swelling.

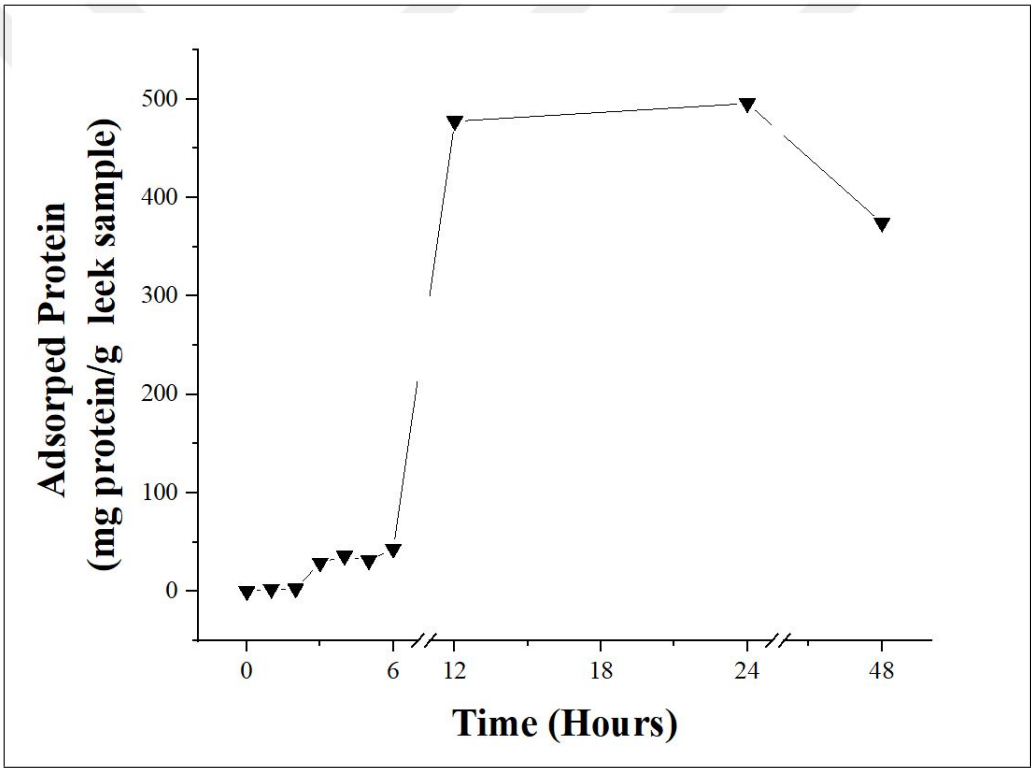


Figure 4.7 Protein adsorption capacity of decellularized leek tissues. Human serum albumin was used as protein solution and leeks were interacted with it for 48 hours. (n=3)

4.3.2 Degradation Behavior

In this thesis, degradation behavior of decellularized leek samples was observed in PBS (pH=7.4) at 37°C. Even though, acidic or alkaline chemicals weren't used for accelerating the process; decellularized leek samples lost approxiamtely 25% of their

total weight in 21 days (Figure 4.8).

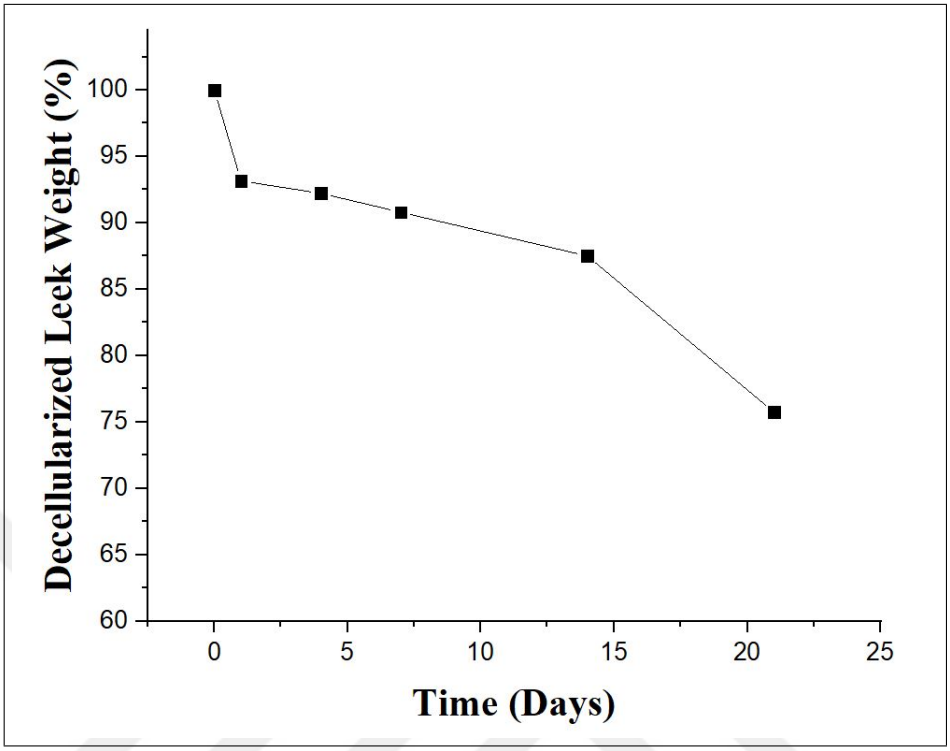


Figure 4.8 Degradation behavior of decellularized leek samples was observed in PBS at pH=7 and 37°C.

4.3.3 Swelling Ratio

Swelling ratio of native leek samples was measured to be 1133.82±11.41% and 1051.17±120.71% in PBS and DMEM, respectively. Decellularized leek samples swelled approximately 2.5 times more in PBS (2411.04±388.45%) and 1.5 times more in DMEM (1564.38 ± 110.97%) than not-treated (native) ones; as it can be seen in Figure 4.9(A). On the other hand, fluid uptake ratio of APTES, OTS modified and GO-coated leek samples were measured to be 1001.89 ± 152.37%, 796.94±179.52%, 843.76±199.51% in PBS; 633.42±15.25%, 610.61±57.99%, 701.40±125.73% in DMEM, respectively [Figure 4.9(B)].

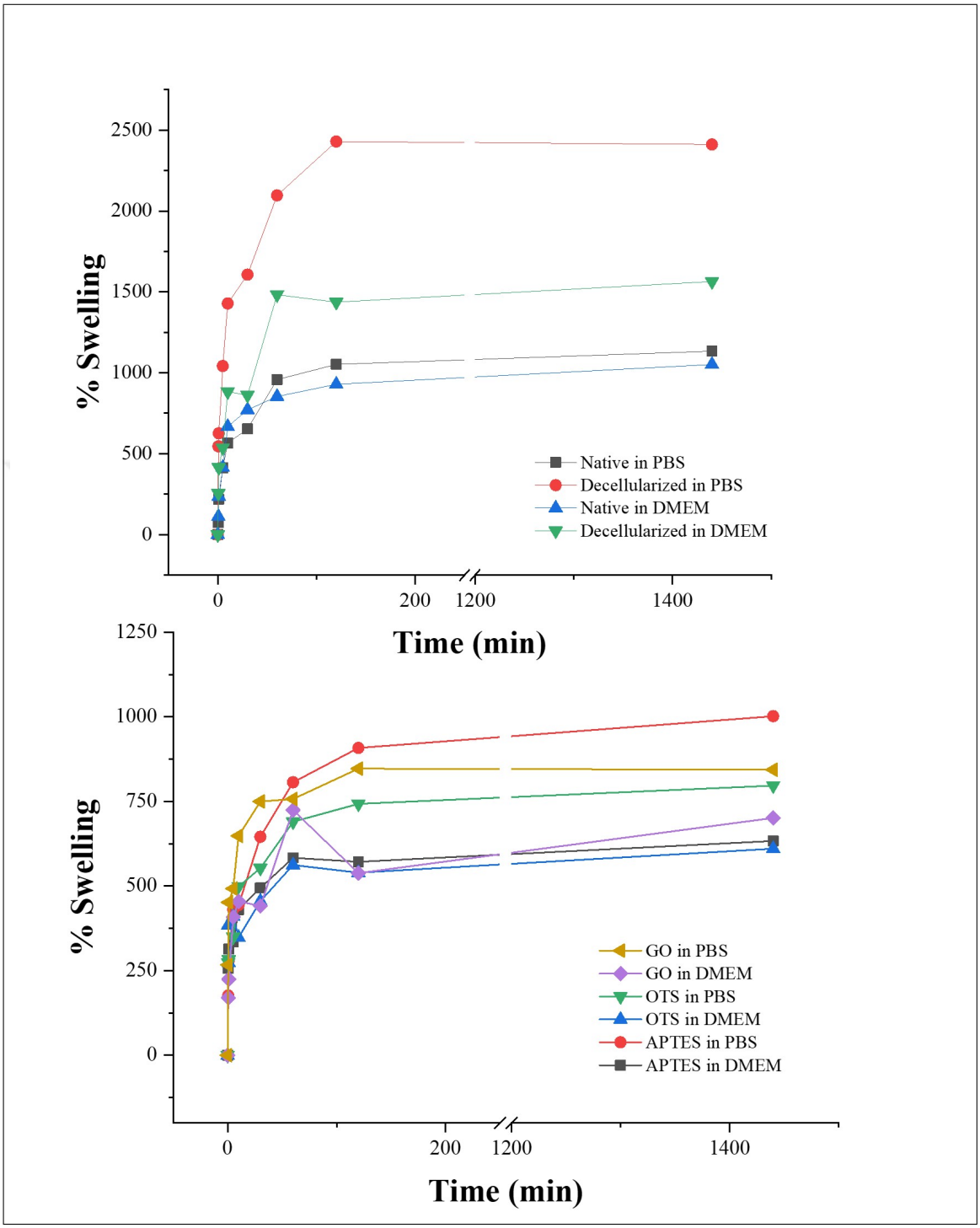


Figure 4.9 Swelling ratios of A. Native and decellularized B. APTES, OTS and GO-modified leek samples in PBS and DMEM at room temperature.

4.3.4 Chemical Analysis

The FT-IR analysis was performed in order to characterize functional groups of native, decellularized, APTES and OTS modified and GO coated leek samples. As seen in Figure 4.10(A), the peak at 1420 cm^{-1} demonstrated C-H and O-H wag in cellulose and hemicellulose. At 1092 cm^{-1} C-O and C-C stretch was observed as well. The peak at 1734 $cm^{-}1$ is the specific band of C=O stretch in functional groups in hemicelluloses [43]. APTES-modification was proved by the peaks of the N-H bond at 1574 cm^{-1}, Si-O-C bond at 1165, 1072, and 952 cm^{-1}, C-NH_2 at 1100 cm^{-1}. Si-O stretching appeared in a broad absorption range of 900-1100 cm^{-1} and 1296 and 764 cm^{-1} indicated the Si-C vibration [44]. Characteristic peaks of OTS appeared at 2870 cm^{-1} for terminal methyl (-CH_3) group vibrations and at 2920 cm^{-1} for its Fermi resonance [45]. GO-coating was proved by the peaks at 1730 and 1639 cm^{-1} that showed C=O stretching and at 1226 and 1044 cm^{-1} that indicated C-O stretching vibrations [Figure 4.10(B)] [46].

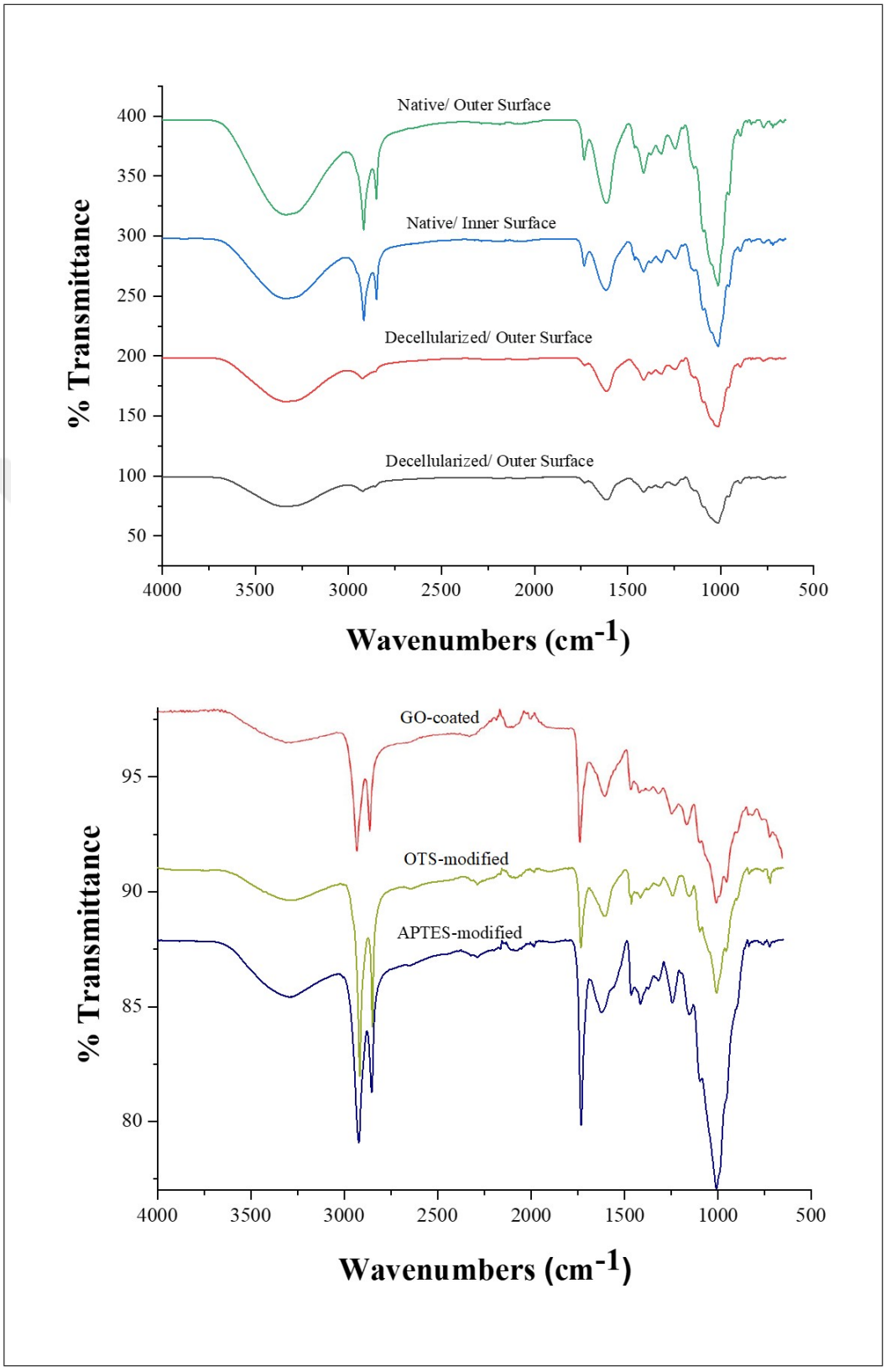


Figure 4.10 FT-IR analysis of A. inner and outer surfaces of native and decellularized B. APTES, OTS modified and GO-coated leek samples.

4.3.5 Mechanical Properties

Mechanical properties of leek samples were analyzed with tensile testing in order to observe the effect of decellularization process. According to these test results as seen on Table 4.1; between native and decellularized leek samples, there is no major difference in stiffness (elastic modulus); 4.05±0.90 kPa and 4.42±0.41 kPa respectively. However, tensile strength of decellularized leek samples slightly increased (1.89±0.25MPa) compared to native samples (1.54±0.28 MPa). The effects of modifications and coating on mechanical properties were also examined. Modified and coated samples became more flexible as their stiffness values diminished (1.31±0.14 kPa for APTES; 0.54±0.14 kPa for OTS; 1.50±0.07 kPa for GO) when compared to unmodified decellularized samples. In terms of tensile strength both APTES modification and GO coating enhanced the physical properties (2.45±0.27 MPa and 1.93±0.10MPa respectively) while OTS modification weakened the material strength (1.08±0.28MPa).

Table 4.1
Mechanical properties of native, decellularized and modified leek samples.

Leek	Stiffness (kPa)	Tensile Strength (MPa)
Native	4.05±1.11	1.54±0.28
Decellularized	4.42±0.50	1.89±0.25
APTES-modified	1.31±0.15	2.45±0.27
OTS-modified	0.54±0.14	1.08±0.28
GO-coated	1.50±0.07	1.93±0.10

4.4 Cell Studies

4.4.1 MTT Cell Viability Assay

In order to investigate the behavior of SH-SY5Y cells on cellulose-based scaffolds; SH-SY5Y cells were seeded on both inner and outer surfaces of decellularized leek samples as well as APTES, OTS modified and GO-coated ones (n=3). According

to MTT cell viability assay (Figure 4.11.), cell viability of GO coated leek samples significantly increased compared to inner and outer surface of decellularized samples also APTES and OTS modified samples.

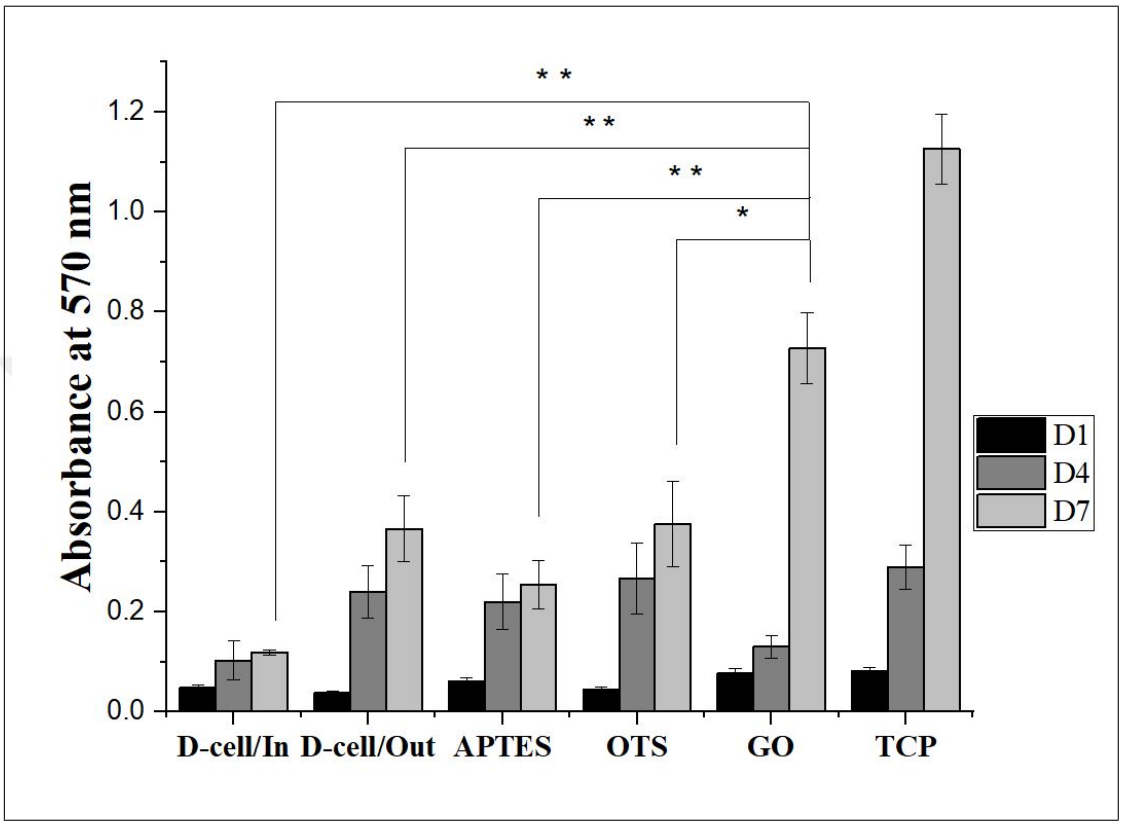


Figure 4.11 MTT cell viability test results for seeded SH-SY5Y cells on both inner and outer surfaces of decellularized leek and APTES, OTS modified and GO-coated decellularized leek samples at day 1,4 and 7 (n=3). (* $p<0.05$, ** $p<0.01$)

4.4.2 Cell Morphology

Behavior of SH-SY5Y cells on decellularized, APTES and OTS modified and GO coated leek samples was observed with SEM analysis (Figure 4.12). Outer surface of decellularized leek samples showed better cell adhesion compared to inner side. Cells started to attach and spread by producing filopodia on the outer surface of decellularized leek samples [Figure 4.12 (C-D)]. Cells were also attached on APTES and OTS modified decellularized leek samples and rounded morphology was observed related to aggregation of cells instead of spreading [Figure 4.12 (F-H)]. Cells that have shown normal neuroblastic morphology tend to spread on GO coated surface by producing

numerous filopodia and lamellipodia in order to adhere and elongate in patterns of leek [Figure 4.12 (I-J)].

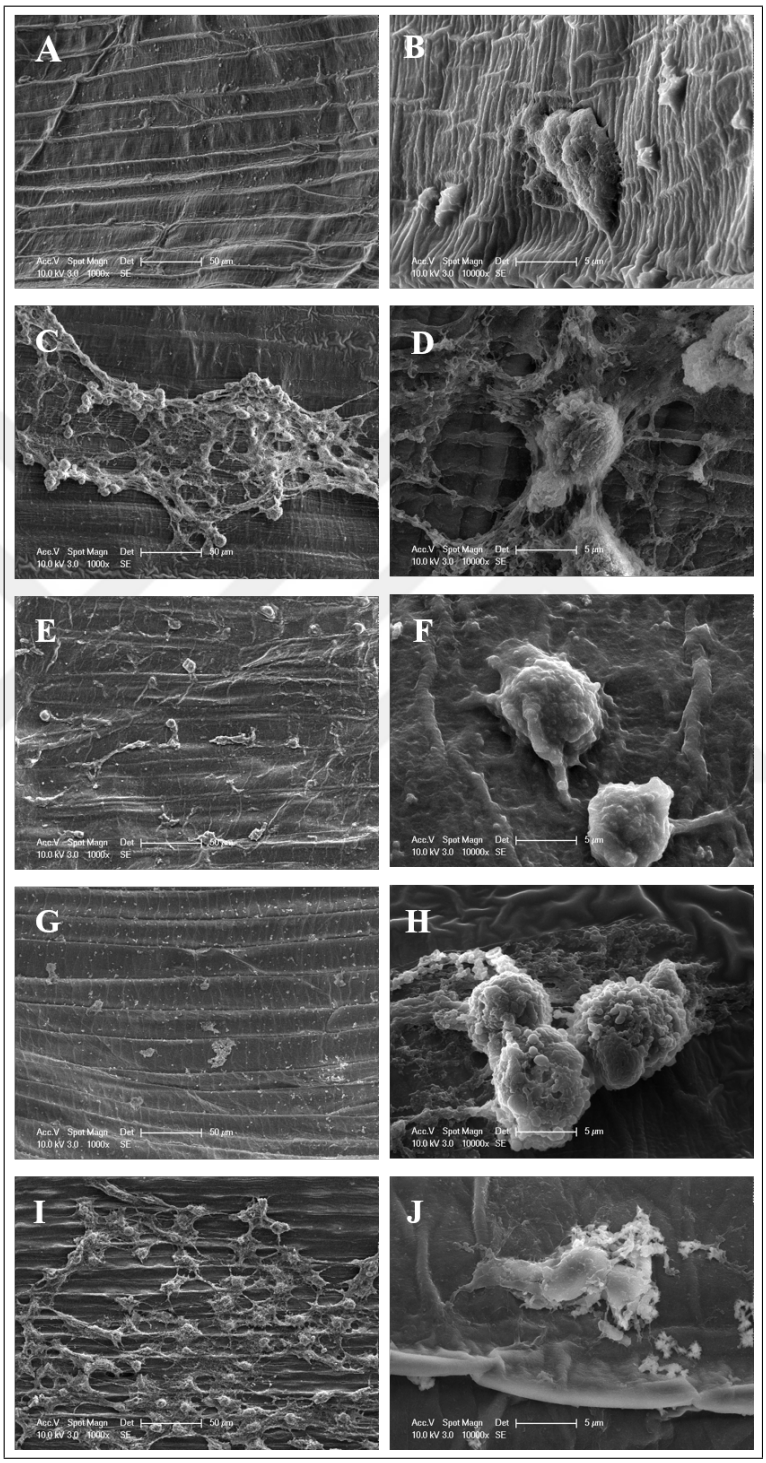


Figure 4.12 SEM images of SH-SY5Y cells seeded decellularized leek samples; inner surface (A-B), outer surface (C-D), APTES-coated surface (E-F), OTS-coated surface (G-H), GO-coated surface (I-J).

5. DISCUSSION

5.1 Decellularization and Characterization of Leek Scaffolds

Mimicry of plant and animal tissues is promising for the future of biomedical applications, especially in tissue engineering by taking advantage of similarities between different structures of these two species as a combination of decellularization of plant and recellularization with mammalian cells. Plants are easily attainable in nature and handling them is cost effective compared to using animal products for repairing damaged tissues. Decellularization of a plant tissue is a simple and rapid method for removing the cellular content and obtaining a scaffold from its remaining extracellular matrix in the form of a cell wall which is made from the polysaccharide cellulose that is the most abundant organic molecule in nature [47].

Leek was chosen for this thesis because of its morphological structure that has been formed by channel-like, elongated and interconnected patterns which provide a platform for SH-SY5Y human neuroblastoma cells to adhere and spread [48]. Cellular content of leek was removed easily with a detergent-like solution within a treatment of 5 days. Leek samples lost their green color and became almost transparent after the 5 days in SDS solution. This is a proof of chlorophyll removal that is the responsible pigment of green colour of several plants [49].

Inner and outer surfaces of decellularized leek samples showed different topographical and chemical characteristics. Hemicellulose is the dominant carbohydrate in the compound middle lamella, which connects the cell walls of two adjoining plant cells together, whereas cellulose is mostly found in the secondary layers of the cell wall [50]. Therefore, the chemical differences between inner and outer surfaces of leek samples can be explained with the amount of hemicellulose, which is abundant at outer surface and cellulose at inner surface. Both inner and outer sides were formed from cellulose that consisted of amorphous and crystalline regions. According to FT-IR analysis

[Figure 4.10(A)] the transmittance at 1420 and 894 cm^{-1} were sensitive the crystalline region of cellulose which were present significantly in native samples [51]. After the decellularization chemical structure became more disordered.

According to SEM images, their patterns and pattern widths were different from each other (23±1.50μm and 17±2.09μm for inner surface; 35±2.90μm and 24±2.07μm for outer surface native and decellularized respectively). Depths of inner and outer surfaces of decellularized leek patterns were measured as approximately 300μm and 50μm respectively with profilometer analysis. In the literature, human neuroblastoma cells were seeded on line patterned PDMS surfaces with different widths (20, 40, 60 and 100 μm) in order to investigate the confinement of cells in patterns while growing [52]. The dimensions of decellularized leek samples are convenient spaces for human neuroblastoma cells to settle and attach according to study of Nam et al. [52].

Degree of decellularization was observed using immunofluorescence staining along with DNA and protein quantifications, to show removal of cellular content. We hypothesized that SDS treatment enables the breakdown of the nuclei, but the inactive contents of nucleus could not be removed from the cell due to the cell wall. In the literature, some studies showed that different decellularization and DNA quantification methods effected the amount of DNA that remained in the structure and even approximately 70% of DNA reduction was accepted for animal tissue decellularization [53]. For plant decellularization, there is only two studies that reported the quantity of reduction in DNA in which J.R. Gershlak et al. demonstrated that decellularized spinach leaves lost almost all of their DNA (9.4±1.3 and 1129±217.3 ng DNA/mg tissue for decellularized and native respectively.) [6]. Spinach leaves are thinner and more brittle structures compared to leek tissues therefore, the removal of nucleus content from cell wall might be easier. In another study, G. Fontana et al. investigated decellularization of several stems and leaves of various plant tissues such as bamboo, orchid, vanilla, anthurium, parsley, calathea and solenostemon and they only provided the DNA quantification data of parsley stem which is approxiamtely 93% [10]. Most probably, they couldn't obtain similar results for other plant tissues due to structural differences. J.R. Gershlak et al. also performed Bradford assay for protein quantifi-

cation and their results showed that spianch leaves lost 87.43% of their total protein content [6]. Protein quantification results of decellularized leek samples showed the same reduction in total protein content (90.37%). It can be hypothesized that remaining 9.63 % of protein quantity was considered to be the membrane proteins that can be found in the extracellular matrix [54]. Therefore, decellularized leek samples can be used as plant-derived cellulose based scaffolds due to majority of plant protein content was removed.

In order to enhance mammalian cell adhesion on decellularized leek scaffolds, different surface modifications were experimented. Organosilanes such as APTES and OTS were chosen for enhancing electrostatic interactions with amino (-NH_2) groups and hydrophobic interactions with methyl (-CH_3) groups respectively. S. Taokaew et al. showed that these organosilanes improved cell attachment on bacterial cellulose [36]. On the other hand, GO coatings were found stable, non-reactive and biocompatible. N. Tasnim et al. demonstrated that GO coated surfaces were sutiable for SH-SY5Y cells to adhere, spread and proliferate, without requiring any neuronal growth factors and showing any significant *in vitro* cytotoxicity [55].

APTES and OTS modifications on the celluose surface were proved by the peaks at 1165, 1072, and 952 cm^{-1} indicated the existence of Si-O-C bond as well as at 1100 cm^{-1} indicated C-NH_2 bond [44]. GO-coating was proved by the peaks at 1730 and 1639 cm^{-1} that showed C=O stretching and at 1226 and 1044 cm^{-1} that indicated C-O stretching vibrations [Figure 4.10(B)] [46].

To the best of our knowledge; swelling and degradation behaviors as well as protein adsorption capacity of decellularized plant tissues were analyzed for the first time in this thesis. After decellularization procedure, because of the removal of cellular content, the fluid uptake capacity was increased, therefore swelling ratio of decellularized samples increased as well. Compared to PBS, leek samples swelled less in DMEM which contains supplementary growth factors that couldn't pass the plant cell wall. Decellularized leek samples swelled 2411.04±388.45% in PBS which is 2.5 times more than native leek samples that swelled 1133.82±11.41%. The same behavior was ob-

served also in decellularized animal tissues such as liver and adipose tissues. M. Song et al. showed that decellularized human adipose tissue swelled 561±19.3% due to high porosity and D.W. Evans et al. who studied liver decellularization, determined that permeability of decellularized tissues was higher than native ones [56],[57]. APTES-modified samples had the highest swelling ratio (1001.89±152.37%) compared to OTS modified (796.94±179.52%) and GO coated samples (843.76±199.51%) that swelled even less when compared to native samples (1051.17±120.71%). Between different modifications, OTS-modified samples showed the lowest swelling property. OTS modification caused hydrophobic behavior and decreased fluid adsorption ratio of cellulosic scaffolds [45]. GO coating increased the swelling ratio due to its hydrophilic functional groups such as -COOH, -OH, -C-O-C and -C=O [58]. In the case of APTES-modified samples, it is known that the degree of crosslinking of APTES molecules changes its swelling behavior. Unreacted, excess APTES on the surface had lower crosslink density that decreased the resistence to swelling therefore, fluid uptake ratio increased [44]. As a result of the change in swelling behavior of the modified samples, it can be argued that swelling ratio can be controlled by surface coatings.

Highly hydrophilic cellulosic surface enriched with -OH groups interacted with amino groups of HSA and formed hydrogen bonds [59]. Protein adsorption on cellulose surfaces were enhanced with increasing contact time in protein solution until equilibrium (12-24h); which showed the compatibility of decellularized leek samples with proteins. After 24 hours, adsorbed protein quantity slightly decreased which indicated that decellularized leek samples released proteins back to the solution. This behavior can be explained by the saturation of binding sites on the cellulosic surfaces [38].

In addition, degradation rate of the cellulose scaffolds was important for clinical applications; it should be long enough for recovery of damaged tissue and short enough not to cause any serious foreign body reaction [2]. In the literature; degradation of cellulose was observed enzymatically (under acidic or alkaline conditions); therefore, our results were not comparable to those studies. However, we hypothesized that drying conditions before the experiment affected the degradation behavior. Presumably, while highly swellable decellularized leek samples were dried in an oven at 60°C; some changes

occurred in the structure and degradation rate was increased. Even so; the degradation behavior of decellularized leek samples under physiological conditions was promising for further studies.

Mechanical properties were tested for both tensile strength and stiffness in order to assess if the decellularization process would result in noticeable changes in the structure or in the physical properties of the leek samples. Looking at the findings, decellularized leek samples did not suffer major changes in terms of their physical properties. Stiffness values were measured 4.05±1.11 kPa and 4.42±0.50 kPa for native and decellularized leek samples respectiveley. Considering the fact that the standard deviation values of the acquired stiffness values were larger than the difference between the stiffness of the native and decellularized samples, it can be argued that the change in stiffness after the decellularization process was negligible. Obtained scaffolds had appropriate mechanical properties for physiological functions in terms of elastic moduli (stiffness) that is ranging from 100 Pa to 100 kPa for human tissues and organs (excluding bone and cartilage) [52]. D.J.Modulevsky et al. who studied apple decellularization obtained similar results in terms of stiffness. They measured stiffness values of apple tissues at 0.9±0.1 kPa, 1.1±0.1 kPa for native and decellularized respectively [9]. J.R. Gershlak et al. showed that spinach leaves had higher stiffness compared to apple and leek tissues however, after decellularization stiffness decreased from 0.8MPa to 0.3MPa [6]. On the other hand, tensile strengths were measured as follows; 1.54±0.28 MPa and 1.89±0.25 MPa for native and decellularized respectively. In the literature, J.R. Gershlak et al. demonstrated that tensile strength values were decreased from 0.15 MPa to 0.05MPa after decellularization of spinach leaves [6]. It is important to note that the change in strength only signifies that the processed materials can facilitate higher amounts of strain. Whereas, the elastic modulus is material specific property which is not related to any parameter such as strain or strength [60].

5.2 Cell Culture Studies

Decellularized leek samples were modified with APTES, OTS and coated with GO prior to cell seeding in order to enhance cell attachment and viability. SH-SY5Y human neuroblastoma cells were seeded and cell viability and behavior were investigated for in terms of the effect of (i) modifications, (ii) geometric constraints and (iii) mechanical properties.

According to MTT results, inner and outer surfaces of decellularized leek samples didn't show any significant difference in terms of cell viability. However, GO coated surfaces showed higher cell viability compared to APTES-OTS modified and non-modified samples. Nevertheless, between APTES and OTS modified surfaces, there weren't any significant statistical differences.

However, SEM images showed the best cell adhesion on GO-coated decellularized leek samples. Cells were attached and started to spread by producing filopodia. Our results agreed with the literature which claimed that GO-coated surfaces promoted cell growth and didn't show any cytotoxic effect [61]. Our results also supported the literature claims which suggest that neuroblastoma cells adhered and proliferated more on GO-coated surfaces in comparison with APTES-coated surfaces [62]. Similar cell adhesion was noticed on outer surface of decellularized leek samples. However, in this case, the effect of pattern morphology came into prominence. Geometric constraints like spatial patterning and their dimensions play major role in growth of neuroblastoma cells [52]. Pattern width of outer surface of decellularized leek was approximately 24$\pm$2.07 μm, which was larger than inner surface patterns (17$\pm$2.09 μm). The number of cells increased with the pattern widths and prolonging of cells restrained along the pattern direction [52]. Cells were also attached as clumps on APTES and OTS modified surfaces however, they couldn't spread.

It's been argued by previous studies that both the pattern and the stiffness of the surface can have significant effects on the cell adhesion and proliferation. There existed an inverse correlation between the cell proliferation and stiffness of extracellu-

lar matrix for neuroblastoma cells. In addition, a stiffness of 3.5 kPa is claimed to be optimal for cell proliferation and stiffness values less than 1 kPa are optimal for differentiation to neurons [63]. After the modification of decellularized leek samples stiffness values decreased to 1.31±0.15 kPa, 0.54±0.14 kPa and 1.50±0.07 kPa for APTES, OTS modification and GO coating, respectively. These surfaces might be favorable for differentiation of neuroblastoma cells to neurons in further studies. With respect to mentioned studies, it can be argued that decellularized leek is a potential suitable substrate for cell adhesion and proliferation in terms of its biomechanical properties.

5.3 Conclusion

Decellularization of plant tissues is a simple and rapid process to obtain cellulose-based 3D scaffolds for tissue engineering applications. Plants are easily attainable in nature and cost effective compared to human donors and animal products as considering for biomaterials. Cellulosic surfaces are biocompatible, and their biomechanical properties can be easily controlled by simple modifications. Our results demonstrated that decellularized and modified leek samples were suitable for *in vitro* mammalian cell culture and potential tissue engineering applications. Standardization of these materials that are derived from nature is the major challenge at this stage of study. For further investigations, immune response and stability should be considered. For all that, plant decellularization is a potential alternative approach for tissue engineering scaffolds according to results that were obtained in this thesis.

5.4 Future Studies

The major challenge of these biological, cellulose-based scaffolds is the standardization of their surfaces. This is the first problem that should be solved by producing them by using biomimetic techniques with materials that have easily adjustable properties. On the other hand, biocompatibility is the basic requirement for scaffold materials.

Therefore, immunomodulation studies should be conducted in order to investigate foreign body reactions and immune responses of cellulosic scaffolds when they interacted with human body.

APPENDIX A. SUPPORTING INFORMATION

A.1 Bradford Protein Quantification Assay

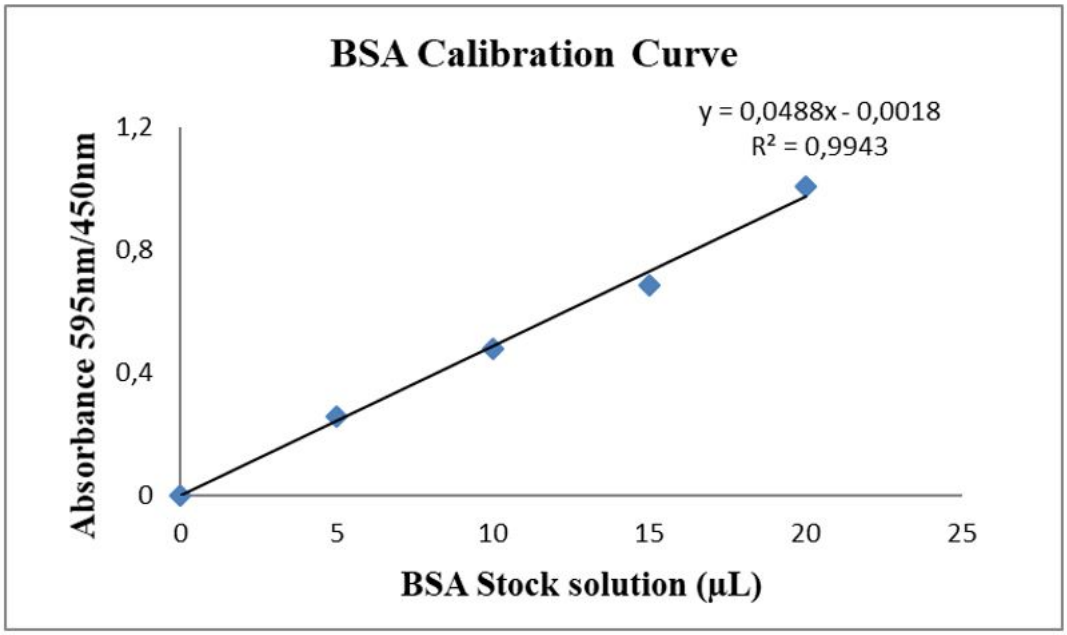


Figure A.1 Calibration curve for Bradford protein quantification assay.

REFERENCES

1. Modulevsky, D. J., C. M. Cuerrier, and A. E. Pelling, "Biocompatibility of Subcutaneously Implanted Plant-Derived Cellulose Biomaterials," *PLoS ONE*, Vol. 11, no. 6, pp. 1–19, 2016.

2. O'Brien, F. J., "Biomaterials & scaffolds for tissue engineering," *Materials Today*, Vol. 14, no. 3, pp. 88–95, 2011.

3. "OPTN/SRTR 2017 Annual Data Report," *American Journal of Transplantation*, Vol. 19, pp. 1–10, 2019.

4. Badylak, S. F., D. Taylor, and K. Uygun, "Whole-organ tissue engineering: Decellularization and recellularization of three-dimensional matrix scaffolds," *Journal of Biomedical Materials Research - Part A*, Vol. 103, no. 4, pp. 1498–1508, 2015.

5. Badylak, S. F., B. N. Brown, and T. W. Gilbert, "Tissue Engineering with Decellularized Tissues," in *Biomaterials Science: An Introduction to Materials: Third Edition*, Vol. 10, pp. 1316–1331, Elsevier, third edit ed., 2013.

6. Gershlak, J. R., S. Hernandez, G. Fontana, L. R. Perreault, K. J. Hansen, S. A. Larson, B. Y. Binder, D. M. Dolivo, T. Yang, T. Dominko, M. W. Rolle, P. J. Weathers, F. Medina-Bolivar, C. L. Cramer, W. L. Murphy, and G. R. Gaudette, "Crossing kingdoms: Using decellularized plants as perfusable tissue engineering scaffolds," *Biomaterials*, Vol. 125, pp. 13–22, 2017.

7. Sindhu, K. A., R. Prasanth, and V. K. Thakur, "Medical Applications of Cellulose and its Derivatives: Present and Future," in *Nanocellulose Polymer Nanocomposites: Fundamentals and Applications*, ch. 16, pp. 437–477, 2014.

8. Bezerra, R. D., P. R. Teixeira, A. S. Teixeira, C. Eiras, J. A. Osajima, and E. C. S. Filho, "Chemical Functionalization of Cellulosic Materials â Main Reactions and Applications in the Contaminants Removal of Aqueous Medium," in *Cellulose - Fundamental Aspects and Current Trends*, ch. 4, pp. 93–113, 2015.

9. Modulevsky, D. J., C. Lefebvre, K. Haase, Z. Al-Rekabi, and A. E. Pelling, "Apple derived cellulose scaffolds for 3D mammalian cell culture," *PLoS ONE*, Vol. 9, no. 5, 2014.

10. Fontana, G., J. Gershlak, M. Adamski, J. S. Lee, S. Matsumoto, H. D. Le, B. Binder, J. Wirth, G. Gaudette, and W. L. Murphy, "Biofunctionalized Plants as Diverse Biomaterials for Human Cell Culture," *Advanced Healthcare Materials*, Vol. 6, no. 8, 2017.

11. Zhao, P., H. Gu, H. Mi, C. Rao, J. Fu, and L. s. Turng, "Fabrication of scaffolds in tissue engineering: A review," *Frontiers of Mechanical Engineering*, Vol. 13, no. 1, pp. 107–119, 2018.

12. Chan, B. P., and K. W. Leong, "Scaffolding in tissue engineering: General approaches and tissue-specific considerations," *European Spine Journal*, Vol. 17, no. SUPPL. 4, 2008.

13. Eltom, A., G. Zhong, and A. Muhammad, "Scaffold Techniques and Designs in Tissue Engineering Functions and Purposes: A Review," *Advances in Materials Science and Engineering*, Vol. 2019, pp. 1–13, 2019.

14. Dhandayuthapani, B., Y. Yoshida, T. Maekawa, and D. S. Kumar, "Polymeric scaffolds in tissue engineering application: A review," *International Journal of Polymer Science*, Vol. 2011, no. ii, 2011.

15. Pallua, N., and C. V. Suschek, "Tissue engineering: From lab to clinic," *Tissue Engineering: From Lab to Clinic*, Vol. 9783642028, pp. 1–634, 2011.

16. Salgado, A. J., O. P. Coutinho, and R. L. Reis, "Bone tissue engineering: State of the art and future trends," *Macromolecular Bioscience*, Vol. 4, no. 8, pp. 743–765, 2004.

17. Rouchi, A. H., and M. Mahdavi-Mazdeh, "Review article," *International Journal of Organ Transplantation Medicine*, Vol. 6, no. 3, 2015.

18. Gilpin, A., and Y. Yang, "Decellularization Strategies for Regenerative Medicine: From Processing Techniques to Applications," *BioMed Research International*, Vol. 2017, pp. 1–13, 2017.

19. Crapo, P. M., T. W. Gilbert, and S. F. Badylak, "An overview of tissue and whole organ decellularization processes," *Biomaterials*, Vol. 32, no. 12, pp. 3233–3243, 2011.

20. Gilbert, T. W., T. L. Sellaro, and S. F. Badylak, "Decellularization of tissues and organs," *Biomaterials*, Vol. 27, no. 19, pp. 3675–3683, 2006.

21. Arenas-Herrera, J. E., I. K. Ko, A. Atala, and J. J. Yoo, "Decellularization for whole organ bioengineering," *Biomedical Materials*, Vol. 8, no. 1, 2013.

22. Simsa, R., A. M. Padma, P. Heher, M. Hellström, A. Teuschl, L. Jenndahl, N. Bergh, and P. Fogelstrand, "Systematic in vitro comparison of decellularization protocols for blood vessels," *PLoS ONE*, Vol. 13, no. 12, pp. 1–19, 2018.

23. Elder, B. D., S. V. Eleswarapu, and K. A. Athanasiou, "Extraction techniques for the decellularization of tissue engineered articular cartilage constructs," *Biomaterials*, Vol. 30, no. 22, pp. 3749–3756, 2009.

24. Schenke-Layland, K., O. Vasilevski, F. Opitz, K. König, I. Riemann, K. J. Halbhuber, T. Wahlers, and U. A. Stock, "Impact of decellularization of xenogeneic tissue on extracellular matrix integrity for tissue engineering of heart valves," *Journal of Structural Biology*, Vol. 143, no. 3, pp. 201–208, 2003.

25. Mhanna, R., and A. Hasan, "Introduction to Tissue Engineering," in *Tissue Engineering for Artificial Organs: Regenerative Medicine, Smart Diagnostics and PersonalizedMedicine*, ch. 1, pp. 3–34, Wiley-VCH, 1sr ed., 2017.

26. Fu, R. H., Y. C. Wang, S. P. Liu, T. R. Shih, H. L. Lin, Y. M. Chen, J. H. Sung, C. H. Lu, J. R. Wei, Z. W. Wang, S. J. Huang, C. H. Tsai, W. C. Shyu, and S. Z. Lin, "Decellularization and recellularization technologies in tissue engineering," *Cell Transplantation*, Vol. 23, no. 4-5, pp. 621–630, 2014.

27. Bourgine, P. E., B. E. Pippenger, A. Todorov, L. Tchang, and I. Martin, "Tissue decellularization by activation of programmed cell death," *Biomaterials*, Vol. 34, no. 26, pp. 6099–6108, 2013.

28. Wang, Y., C. T. Nicolas, H. S. Chen, J. J. Ross, S. B. De Lorenzo, and S. L. Nyberg, "Recent Advances in Decellularization and Recellularization for Tissue-Engineered Liver Grafts," *Cells Tissues Organs*, Vol. 203, no. 4, pp. 203–214, 2017.

29. Lodish, H., A. Berk, and S. Zipursky, "The Dynamic Plant Cell Wall," in *Molecular Cell Biology* (Freeman, W., ed.), ch. 22.5, 4th ed., 2000.

30. Fang, S., L. Li, B. Cui, S. Men, Y. Shen, and X. Yang, "Structural insight into plant programmed cell death mediated by BAG proteins in Arabidopsis thaliana," *Acta Crystallographica Section D: Biological Crystallography*, Vol. 69, no. 6, pp. 934–945, 2013.

31. Wasteneys, G. O., J. Willingale-Theune, and D. Menzel, "Freeze shattering: a simple and effective method for permeabilizing higher plant cell walls," *Journal of Microscopy*, Vol. 188, pp. 51–61, 1997.

32. Musielak, T. J., L. Schenkel, M. Kolb, A. Henschen, and M. Bayer, "A simple and versatile cell wall staining protocol to study plant reproduction," *Plant Reproduction*, Vol. 28, no. 3-4, pp. 161–169, 2015.

33. Zangala, T., "Isolation of Genomic DNA from Mouse Tails," *Journal of Visualized Experiments*, Vol. 2463791, no. 6, p. 246, 2007.

34. Ernst, O., and T. Zor, "Linearization of the Bradford Protein Assay," *Journal of Visualized Experiments*, no. 38, pp. 1–6, 2010.

35. Khanjanzadeh, H., R. Behrooz, N. Bahramifar, W. Gindl-Altmutter, M. Bacher, M. Edler, and T. Griesser, "Surface chemical functionalization of cellulose nanocrystals by 3-aminopropyltriethoxysilane," *International Journal of Biological Macromolecules*, Vol. 106, pp. 1288–1296, 2018.

36. Taokaew Siriporn Phisalaphong, Muenduen Newby, B.-m. Z. S., "Modification of bacterial cellulose with organosilanes to improve attachment and spreading of human fibroblasts," *Cellulose*, Vol. 22, no. 4, pp. 2311–2324, 2015.

37. Yan, T., H. Zhang, D. Huang, S. Feng, M. Fujita, and X.-D. Gao, "Chitosan-Functionalized Graphene Oxide as a Potential Immunoadjuvant," *Nanomaterials*, Vol. 7, no. 3, p. 59, 2017.

38. Mujtaba, M., I. Sargin, and M. Kaya, "Determination of Bovine Serum Albumin Adsorption Capacity of Newly Obtained Cellulose extracted from Glycyrrhiza glabra (Licorice)," *Advances in Polymer Technology*, Vol. 37, no. 2, pp. 606–611, 2018.

39. Zhang, H., L. Zhou, and W. Zhang, "Control of Scaffold Degradation in Tissue Engineering: A Review," *Tissue Engineering Part B: Reviews*, Vol. 20, no. 5, pp. 492–502, 2014.

40. Cai, Z., and J. Kim, "Preparation and Characterization of Novel Bacterial Cellulose/Gelatin Scaffold for Tissue Regeneration Using Bacterial Cellulose Hydrogel," *Journal of Nanotechnology in Engineering and Medicine*, Vol. 1, no. 021002, pp. 1–6, 2010.

41. Kovalevich, J., and D. Langford, "Considerations for the Use of SH - SY5Y Neuroblastoma Cells in Neurobiology," in *Neuronal Cell Culture Methods and Protocols Methods in Molecular Biology* (Amini, S., and M. K. White, eds.), pp. 9–21, Springer, 2013.

42. Lilly, E., G. Sitta Sittampalam, N. P. Coussens, K. Brimacombe Abigail Grossman, M. Arkin, D. Auld, C. Austin Jonathan Baell, B. Bejcek, J. M. Caaveiro Thomas DY Chung, J. L. Dahlin, V. L. Devanaryan Timothy Foley, M. Glicksman, M. D. Hall Joseph V Haas, J. Inglese, P. W. Iversen, S. D. Kahl Stephen C Kales, M. Lal-Nag, Z. Li, J. McGee Owen McManus, T. Riss, O. Joseph Trask, J. R. Weidner Mary Jo Wildey,

M. Xia, and X. Xu, "National Institutes of Health. Assay Guidance Manual," no. Md, 2004.

43. Pucetaite, M., *Archaeological wood from the Swedish warship Vasa studied by infrared microscopy*. PhD thesis, Lunds University, 2012.

44. Mathialagan, M., and H. Ismail, "Polyvinyl Alcohol-Modified Pithecellobium Clypearia Benth Herbal Residue FiberPolypropylene Composites," *Polymer Composites*, Vol. 37, no. 1, pp. 915–924, 2016.

45. Kumar, A., P. Ryparová, A. S. Škapin, M. Humar, M. Pavlič, J. Tywoniak, P. Hajek, J. Žigon, and M. Petrič, "Influence of surface modification of wood with octadecyltrichlorosilane on its dimensional stability and resistance against Coniophora puteana and molds," *Cellulose*, Vol. 23, no. 5, pp. 3249–3263, 2016.

46. Rattana, T., S. Chaiyakun, N. Witit-Anun, N. Nuntawong, P. Chindaudom, S. Oaew, C. Kedkeaw, and P. Limsuwan, "Preparation and characterization of graphene oxide nanosheets," *Procedia Engineering*, Vol. 32, pp. 759–764, 2012.

47. Alberts B, Johnson A, L. J.-e. a., "The Plant Cell Wall," in *Molecular Biology of Cell*, New York: Garland Science, 4th ed., 2002.

48. Robb, K. P., A. Shridhar, and L. E. Flynn, "Decellularized Matrices As Cell-Instructive Scaffolds to Guide Tissue-Specific Regeneration," *ACS Biomaterials Science & Engineering*, p. acsbiomaterials.7b00619, 2017.

49. Heaton, J. W., and A. G. Marangoni, "Chlorophyll degradation in processed foods and senescent plant tissues," *Trends in Food Science & Technology*, Vol. 7, 1995.

50. M.T., H., "Hemicelluloses," *Encyclopedia of Food Sciences and Nutrition*, pp. 3060–3071, 2003.

51. Fan, M., D. Dai, and B. Huang, "Fourier Transform Infrared Spectroscopy for Natural Fibres," in *Fourier Transform - Materials Analysis* (Salih, S., ed.), ch. 3, InTech, 2012.

52. Nam, K. H., N. Jamilpour, E. Mfoumou, F. Y. Wang, D. D. Zhang, and P. K. Wong, "Probing mechanoregulation of neuronal differentiation by plasma lithography patterned elastomeric substrates," *Scientific Reports*, Vol. 4, pp. 1–9, 2014.

53. Antons, J., M. G. Marascio, P. Aeberhard, G. Weissenberger, N. Hirt-Burri, L. A. Applegate, P. E. Bourban, and D. P. Pioletti, "Decellularised tissues obtained by a CO2-philic detergent and supercritical CO2," *European Cells and Materials*, Vol. 36, pp. 81–95, 2018.

54. Jamet, E., H. Canut, G. Boudart, and R. F. Pont-Lezica, "Cell wall proteins: A new insight through proteomics," *Trends in Plant Science*, Vol. 11, no. 1, pp. 33–39, 2006.

55. Tasnim, N., A. Kumar, and B. Joddar, "Attenuation of the in vitro neurotoxicity of 316L SS by graphene oxide surface coating," *Materials Science and Engineering C*, Vol. 73, pp. 788–797, 2017.

56. Song, M., Y. Liu, and L. Hui, "Preparation and characterization of acellular adipose tissue matrix using a combination of physical and chemical treatments," *Molecular Medicine Reports*, Vol. 17, no. 1, pp. 138–146, 2018.

57. Evans, D. W., E. C. Moran, P. M. Baptista, S. Soker, and J. L. Sparks, "Scale-dependent mechanical properties of native and decellularized liver tissue," *Biomechanics and Modeling in Mechanobiology*, Vol. 12, no. 3, pp. 569–580, 2013.

58. Huang, Y., M. Zeng, J. Ren, J. Wang, L. Fan, and Q. Xu, "Preparation and swelling properties of graphene oxide/poly(acrylic acid-co-acrylamide) super-absorbent hydrogel nanocomposites," *Colloids and Surfaces A: Physicochemical and Engineering Aspects*, Vol. 401, pp. 97–106, 2012.

59. Nina E. Kotelnikova, Olga V. Lashkevich, E. F. P., "Mutual Effect of the Interaction of Human Serum Albumin with Cellulose in Water," *Macromol. Symp.*, Vol. 166, pp. 147–156, 2001.

60. Callister, W. D. J., and D. G. Rethwisch, *Fundamentals of Materials Science and Engineering: An Integrated Approach*, John Wiley & Sons, 4 ed., 2012.

61. Wang, B., P. G. Luo, K. N. Tackett II, O. N. Ruiz, and Y.-P. Sun, "Graphene Oxides as Substrate for Enhanced Mammalian Cell Growth," *Journal of Nanomaterials & Molecular Nanotechnology*, Vol. 01, no. 02, pp. 2–5, 2013.

62. Nishat Tasnim, Alok Kumar, B. J., "Attenuation of the In Vitro Neurotoxicity of 316L SS by Graphene Oxide Surface Coating," *Mater Sci Eng C Mater Biol Appl.*, Vol. 73, pp. 788–797, 2017.

63. Lam, W. A., L. Cao, V. Umesh, A. J. Keung, S. Sen, and S. Kumar, "Extracellular matrix rigidity modulates neuroblastoma cell differentiation and N-myc expression," *Molecular Cancer*, Vol. 9, pp. 1–7, 2010.